NASA CONTRACTOR REPORT

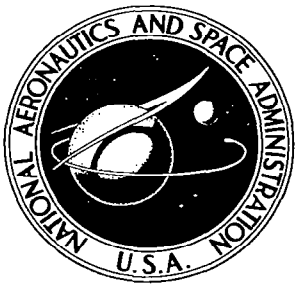

A REVIEW OF ANALYTICAL METHODS USED TO DETERMINE THE MODAL CHARACTERISTICS OF CYLINDRICAL SHELLS

by Kevin Forsberg

Prepared by
LOCKHEED AIRCRAFT CORPORATION
Palo Alto, Calif.

NATIONAL AERONAUTICS AND SPACE ADMINISTRATION • WASHINGTON, D. C. • SEPTEMBER 1966

A REVIEW OF ANALYTICAL METHODS USED TO DETERMINE THE MODAL CHARACTERISTICS OF CYLINDRICAL SHELLS

By Kevin Forsberg

Presented at the

7th International Aeronautical Congress (7th C. I. Aé.)

14-17 June 1965

Paris, France

This work was sponsored by the LMSC Independent Research Program.

Research Laboratories
LOCKHEED MISSILES AND SPACE COMPANY
Palo Alto, Calif.

NATIONAL AERONAUTICS AND SPACE ADMINISTRATION

For sale by the Clearinghouse for Federal Scientific and Technical Information
Springfield, Virginia 22151 – Price $2.50

A REVIEW OF ANALYTICAL METHODS USED TO DETERMINE THE MODAL CHARACTERISTICS OF CYLINDRICAL SHELLS

By Kevin Forsberg*

ABSTRACT

Most authors have used approximate methods to determine the dynamic behavior of cylindrical shells. A recent paper by the present author has discussed results obtained by an exact solution of the differential equations of motion as derived by Flügge. By this method one can determine the modal characteristics of a thin-walled cylindrical shell having arbitrary homogeneous boundary conditions. Thus for the cylindrical shell it is now possible to examine solutions obtained by various approximate techniques, using the exact solution as a basis of comparison. Results obtained by energy and finite difference techniques, as well as exact solutions for simplified (Donnell) differential equations, are compared. The effect of omitting inplane inertia is also examined. The comparisons are made on the basis of natural frequency, mode shape, and modal force distribution, and an indication is given of the time required for solution by the different methods on a high-speed digital computer. This review has considerable importance in providing a means to guide the investigator in making an appropriate choice of method for solving problems in dynamic response of spacecraft structures for which the exact solution is not available or is too cumbersome for his needs.

*Research Specialist, Aerospace Sciences Laboratory, Lockheed Missiles and Space Company, Palo Alto, California, U.S.A.

LIST OF SYMBOLS

a	Radius of cylinder
h	Thickness of cylinder wall
k	$h^2/12a^2$
ℓ	Length of cylinder
m	Number of axial half-waves
n	Number of circumferential waves
u, v, w	Longitudinal, tangential, and radial displacement components
x	Dimensionless axial coordinate, ξ/a
E	Young's Modulus of Elasticity
M_x , $M_{x\varphi}$, M_φ N_x , Q_x , etc.	Stress Resultants (See Fig. 1)
$\tilde{M}_x$, $\tilde{M}_\varphi$	$[12a(1-\nu^2)/Eh^3]\, M_x$; $[12a(1-\nu^2)/Eh^3]\, M_\varphi$
$\tilde{N}_x$, $\tilde{N}_\varphi$	$[(1-\nu^2)/Eh]\, N_x$; $[(1-\nu^2)/Eh]\, N_\varphi$
T_x	$N_x - M_{x\varphi}/a$
δ_j	Ratio of frequency from approximate solution to Ω_e
γ^2	$\rho a^2 (1-\nu^2)/E$
ν	Poisson's ratio
ξ	Axial coordinate
ρ	Mass density of shell material
ρ_o	"Inplane mass density"; $\rho_o = \rho$ if inplane inertia is included, otherwise $\rho_o = 0$
φ	Circumferential coordinate
ω	Circular frequency
ω_o	Lowest extensional frequency of a ring in plane strain, $= 1/\gamma$
Ω_e	Frequency ratio ω/ω_o derived from the Flügge equations, including inplane inertia
$(\ldots)'$	$\partial(\ldots)/\partial x$
$(\ldots)^{\cdot}$	$\partial(\ldots)/\partial\varphi$
$\nabla^4(\ldots)$	$(\partial^2/\partial x^2 + \partial^2/a\partial\varphi^2)^2(\ldots)$
$\nabla^8(\ldots)$	$\nabla^4\nabla^4(\ldots)$

INTRODUCTION

In recent years there has been a trend toward the construction of very large, very flexible structures. It has become increasingly important to accurately define the dynamic behavior of these structures (such as spacecraft) since, among other things, the dynamic response of a flexible structure may contribute significantly to the internal loads. There is need for a description of the dynamic behavior which is more sophisticated than that provided by the lumped mass-spring approach. One of the more promising methods for describing the overall vehicle elastic response is based upon the modal characteristics* of the individual structural elements (which for space vehicles are predominantly thin shells). The success of such a method relies, of course, on having an adequate description of the modal behavior of the various components. In addition to the direct use of the modal characteristics of thin shells, knowledge and understanding of such dynamic behavior is of immense value in analyzing composite structural components of space vehicles, e.g. liquid-filled cylindrical shells or filament-wound cylinders. The present review will discuss various approaches for determining the modal characteristics of a single shell geometry (thin-walled cylinder) and will compare the advantages and disadvantages as well as the relative accuracy of different methods.

In a recent paper [1]**, the present author has discussed results obtained by an exact solution of the differential equations of motion as derived by Flügge [2] for thin-walled isotropic cylindrical shells. By this method one can solve for the modal characteristics of a thin-walled cylinder having arbitrary homogeneous boundary conditions. The method, which was outlined by Flügge in 1934, requires numerical evaluation of an eighth-order determinant to find its eigenvalues, and this is certainly the reason this approach was not feasible before the advent of a high-speed digital computer. Although the method requires numerical computation, the results are exact, in the same sense that the numerical solution to the transcendental frequency equation for a beam yields an exact solution.

* The term "modal characteristics" includes all of the parameters which characterize the modal behavior of a structure, e.g. natural frequency, mode shape, generalized mass, internal modal forces, etc.

**Numbers in brackets refer to references at the end of the paper.

Since an exact solution is available for cylinders, one may ask why approximate techniques need be pursued further for this problem. The exact solution described above can easily be extended to handle a tandem series of cylinders (of different wall thicknesses, if desired), and by introducing ring characteristics (both stiffness and inertia) into the boundary conditions, one has an exact solution for the modal characteristics of a ring-stiffened cylindrical shell. The extension of the method to handle orthotropic shells is also straight-forward. In short, this method will apply to a wide range of engineering problems. However, one must have a reasonable initial estimate (within 30 percent) for the natural frequency in order for this approach to work. The evaluation of the frequency spectrum for a given problem is somewhat cumbersome, and is by no means automatic. An approximate solution, even for a simplified set of differential equations, would be of considerable value for engineering use even though the exact solution is available. It is also clear that there are many problems of engineering interest which can only be solved by approximate techniques (e.g., cylinders having non-uniform wall thickness, non-uniform mass distribution, cutouts, or concentrated masses). It is of considerable interest, then, to have some indication of the limitations of these approximations. The purpose of the present paper is to make a detailed comparison of various approximations in the limiting case of an isotropic thin-walled cylinder, using the exact solution as a base.

There are two distinct phases of this problem which must be discussed:
(1) approximations made in formulation of the equations of motion, and
(2) approximations made in solving these equations. One can make certain simplifications in the formulation of the basic shell equations and obtain a Donnell-type set of equations of motion. Omission of inplane inertia terms will further simplify the problem. One could then find the exact solution to this approximate set of equations. One phase of the present study will investigate the error encountered in such an approach. A second--and distinctly different--error is introduced when one uses an approximate method to solve a selected set of equations of motion. In order to assess this error two approximate methods of solution (minimization of energy and finite difference) will be studied. The results of the two phases of this study will provide a guide as to the magnitude of the error

to be expected when using a specific approach; however, care must be taken in drawing conclusions from these results if the geometry for a given problem differs significantly from that of an isotropic cylindrical shell.

The differential equations used in the present analysis are based on the usual assumptions of linear thin shell theory, i.e., that the shell is thin (usually considered to mean $a/h > 10$), of constant wall thickness, and of a linear, homogeneous, isotropic material. The results apply only for small deflections and, since the effects of shear distortion and rotatory inertia of the shell wall have been neglected, the results apply only when the half-wave length of the mode shape is much larger than the shell wall thickness (usually considered to mean $\ell/ma > 10\ h/a$, $\pi/n > 10\ h/a$, where m and $2n$ are the number of axial and circumferential half waves). The limitations of thin shell theory are discussed in more detail by Greenspon [3].

A sketch of an isotropic cylindrical shell and shell element, depicting the coordinate system as well as the internal forces, is given in Fig. 1. The physical significance of the parameters n and m , which define the nodal pattern on the shell, is indicated in Fig. 2. The nodal lines indicated in Fig. 2 are not nodes in the usual sense of the word; they indicate lines along which two of the three displacement components (u, v, w) are zero. In general the third displacement component will be a maximum along this same line.

EQUATIONS OF MOTION

Flügge Equations

Many investigators (Love, Flügge, Naghdi, Timoshenko, Koiter, Novozhilov, Vlashov, and others) have developed differential equations describing the behavior of thin shells. In a rather general way one can say that the wide variety in the resulting equations arises basically from small differences in the formulation of the strain-displacement relationships, and the discrepancies occur only in terms which numerically have little significance. As long as the limitations of thin shell theory are observed, the various formulations give identical numerical results within engineering accuracy [3, 4]. The equations of motion developed by Flügge [2] are used here as the basis of comparison in evaluation of various approximations. These equations of motion for cylindrical shells are given below:

$$u'' + \frac{1-\nu}{2}(1+k)\,u^{\cdot\cdot} + \frac{1+\nu}{2}\,v'^{\cdot} - kw''' + \frac{1-\nu}{2}\,kw'^{\cdot\cdot} + \nu w' - \gamma^2 \frac{\partial^2 u}{\partial t^2} = 0$$

$$\frac{1+\nu}{2}\,u'^{\cdot} + v^{\cdot\cdot} + \frac{1-\nu}{2}(1+3k)\,v'' - \frac{3-\nu}{2}\,kw''^{\cdot} + w^{\cdot} - \gamma^2 \frac{\partial^2 v}{\partial t^2} = 0$$

$$-ku''' + \frac{1-\nu}{2}\,ku'^{\cdot\cdot} + \nu u' - \frac{3-\nu}{2}\,kv''^{\cdot} + v^{\cdot} + w + k\left[w^{IV} + 2w''^{\cdot\cdot} + w^{\cdot\cdot\cdot\cdot} + 2w^{\cdot\cdot} + w\right] + \gamma^2 \frac{\partial^2 w}{\partial t^2} = 0 \qquad (1)$$

where

$$(\,)' = \frac{\partial(\,)}{\partial x}\,, \qquad (\,)^{\cdot} = \frac{\partial(\,)}{\partial \varphi}$$

$$\gamma^2 = \frac{\rho a^2 (1-\nu^2)}{E}\,, \qquad k = \frac{h^2}{12a^2}$$

The omission of inplane inertia terms ($\gamma^2\,\partial^2u/\partial t^2$, $\gamma^2\partial^2v/\partial t^2$) is one assumption often made in an attempt to simplify the analysis of the dynamic behavior of shells. There is no reason, of course, to omit these terms if one solves the problem exactly as outlined below. Re-solving Eqs. (1) by the exact approach after neglecting inplane inertia, however, allows a unique opportunity to establish numerically the ranges in which these terms are important. The significance of inplane (or tangential) inertia terms has been investigated by Ivaniuta and Finkel'shtein [5], but their evaluation, based on the simplified (Donnell) equations, was limited to a discussion of the variation of the natural frequency for a "freely-supported" shell. The present investigation will be an extension of and addition to their work.

Simplified (Donnell) Equations

The wide variety of differential equations for shells generally disagree only in terms which have little influence. The Donnell-type equations are an exception, however, in that simplifications are made which yield more manageable equations, but which limit the range of applicability of the results.

If one assumes that the thickness to radius ratio h/a is negligible compared to unity*, then one can simplify the basic strain-displacement relationships. Using these simplified expressions one can ultimately derive the set of differential equations first published by Donnell in 1933 in a study of the stability of a cylindrical shell. This simplified set of equations of motion for a cylindrical shell can be readily obtained from the open literature (e.g. Ref 2, p. 220):

$$
\begin{aligned}
&u'' + \frac{1-\nu}{2}\,u^{\cdot\cdot} + \frac{1+\nu}{2}\,v'^{\cdot} + \nu w' - \gamma^2\,\frac{\partial^2 u}{\partial t^2} = 0\\
&\frac{1+\nu}{2}\,u'^{\cdot} + v^{\cdot\cdot} + \frac{1-\nu}{2}\,v'' + w^{\cdot} - \gamma^2\,\frac{\partial^2 v}{\partial t^2} = 0\\
&\nu u' + v^{\cdot} + w + k\,[w^{IV} + 2w''^{\cdot\cdot} + w^{\cdot\cdot}] + \gamma^2\,\frac{\partial^2 w}{\partial t^2} = 0
\end{aligned}
\qquad (2)
$$

*The Donnell equations can be developed in various ways, some of which require assumptions about the magnitude of the circumferential wave length; however, by starting from the exact formulation for the strain at any point in the shell wall, one only needs to assume consistently that $(1+z/a) \simeq 1$, where $-h/2 \le z \le h/2$, in order to arrive at the Donnell equations (see Ref 2, p 216).

One can re-arrange Eqs. (2) so as to yield one equation in w along with two supplementary differential equations relating u and v to w. The advantage of neglecting the inplane inertia terms ($\gamma^2 \partial^2 u/\partial t^2$, $\gamma^2 \partial^2 v/\partial t^2$) is that one obtains a significant simplification in the resulting expression for w, and obtains the more common form for the Donnell equations (the supplementary equations for u and v, although essential for the complete solution of the problem, are not recorded here):

$$a^4 \, k \, \nabla^8 w + (1-\nu^2) \frac{\partial^4 w}{\partial x^4} + \gamma^2 \nabla^4 \frac{\partial^2 w}{\partial t^2} = 0 \qquad (3)$$

These equations have enjoyed wide usage because they can be manipulated more easily than Eqs. (1), and thus are more amenable to approximate analytic solutions. Equations very similar to these have been developed for other geometric shapes such as the cone; the same basic assumptions are essential in formulating more extensive analyses to describe the non-linear behavior of cylindrical shells. Clearly Donnell-type equations are a common and essential tool in static, dynamic, and stability analyses of shells. The range of applicability has been extensively discussed in the literature for static and stability problems (c.f. Ref. 6). To date a similar comparison for the dynamics problem has been lacking. The results contained herein are a first step towards filling this need.

The major attraction of the Donnell equations of motion is their simplicity as compared with Eqs. (1). However a closed form solution has not been available in the past, even for Eqs. (3), except in special cases. It is possible to solve the Donnell equations in general by a number of different approaches; e.g., by an energy method, by finite differences, by asymptotic expansions. However we are interested here in determining the error introduced by the assumptions underlying Eqs. (2) and (3) as compared with Eqs. (1), and hence we do not want to become entangled in additional errors introduced by approximate solutions. For comparative purposes, then, the Donnell equations, both with and without inplane inertia (Eqs. (2) and (3)), have been solved using the exact method. It should be noted that the Flügge and Donnell equations can be handled with equal ease by the exact method, and thus except for purposes of comparison there is little reason to use the Donnell equations if one is going to the trouble to develop the exact solution as outlined below.

METHODS OF SOLUTION

Exact Solution

The exact analysis is based on the equations of motion developed by Flügge [2] for free vibrations of thin, circular cylindrical shells. The method of solution, which is discussed in detail in Ref. 1, is outlined briefly below. The Donnell equations of motion are also solved by this method for comparison.

For a complete cylinder, the general solution for modal vibration can easily be written in the following form

$$
\begin{aligned}
u &= \left(\sum_{s=1}^{8} \alpha_s A_s e^{\lambda_s x} \cos n\varphi \right) e^{i\omega t} \\
v &= \left(\sum_{s=1}^{8} \beta_s A_s e^{\lambda_s x} \sin n\varphi \right) e^{i\omega t} \\
w &= \left(\sum_{s=1}^{8} A_s e^{\lambda_s x} \cos n\varphi \right) e^{i\omega t}
\end{aligned} \tag{4}
$$

Substitution of these expressions into the homogeneous differential equations leads to an eighth-order algebraic equation for λ_s

$$
\lambda_s^8 + g_{s6} \lambda_s^6 + g_{s4} \lambda_s^4 + g_{s2} \lambda_s^2 + g_{s0} = 0 \tag{5}
$$

where

$$
g_{sk} = g_{sk} (h/a , \nu , n , \omega) .
$$

Once the boundary conditions are specified (four at each end of the shell), the problem is entirely determined. The detailed statement of these conditions leads directly to eight simultaneous algebraic equations for the eight unknown constants A_s . These equations involve the eight roots of λ_s . Since the boundary conditions are homogeneous, the determinant D of these equations must be zero for a non-trivial solution.

At this point in the analysis, a numerical evaluation of the solution is introduced. We now select a given shell (i.e., fix a/h, ℓ/a, ν), an assumed number of circumferential waves n, and a specific set of boundary conditions at each end. Starting from some initial estimate for the frequency ω, we can iterate to find the values of ω which will make the determinant D go to zero. We can cover the entire range of problems of interest by varying the initial input to the determinant, i.e. by varying a/h, ℓ/a, ν, n, or the boundary conditions.

No assumptions or simplifications beyond those underlying Eqs. (1) have been introduced in the numerical evaluation, and the solution can be obtained with any desired degree of accuracy.

Finite Difference Approach

An alternative method for describing the modal behavior of a cylindrical shell is to replace the differential equations by a set of difference equations which are defined at a selected number of grid points. The finite difference scheme, along with other closely related methods such as the finite element approach, is widely used because, with this approach, one can handle very complex systems (e.g., a cylindrical shell with a variable wall thickness or with a cutout). In general the differential equations must be replaced by a two-dimensional finite difference scheme, which results in a large number of variables even for a rather coarse grid. However, for a complete shell, it is often possible to write the displacement functions in the form

$$u = \tilde{u}(x) \cos n\varphi \, e^{i\omega t} \tag{6}$$

with similar forms for v and w. Substitution of such expressions into the basic partial differential equations of motion yields a set of ordinary differential equations with the independent variable x. These can then be replaced by a set of one dimensional finite difference equations, and thus with a reasonable number of grid points one can obtain an accurate representation of the shell behavior.

In the present paper Eqs. (1) are used as the basis for the finite difference analysis. All terms, including the three inertia terms, have been retained. The expressions for the stress resultants, used both in the boundary conditions and in computing stresses in the interior of the shell, are based on Flügge's formulation. A sinusoidal variation of the stresses and displacements is assumed in the circumferential direction, as indicated in Eq. (6). The derivatives in the axial direction are approximated by a central difference scheme; the largest derivative is of the fourth order. Once the boundary conditions are specified (the present formulation will handle any set of homogeneous boundary conditions), one obtains a set of simultaneous equations in the form of a standard matrix eigenvalue problem

$$Ax - \left(\frac{\omega}{\omega_o}\right)^2 Ix = 0 \tag{7}$$

where I is a unit matrix.

The matrix A is essentially a diagonal matrix having non-zero elements in as many as eight columns on either side of the diagonal. The "power method" or iterated vector method [7] is used to compute the eigenvalues and eigenvectors. The program is arranged so that the lowest eigenvalue is obtained first, and the matrix is iterated (starting with some assumed eigenvector) until the eigenvalue $(\omega/\omega_o)^2$ is obtained with the desired degree of accuracy.

In the power method the eigenvalues must be found in numerical sequence, i.e. to evaluate the frequency for $m = 5$, one must know the eigenvalues and vectors for the four lower modes. To obtain eigenvalues higher than the first, the eigenvector must be orthogonal to all previous eigenvectors. It has been found that for practical purposes the trial vector must be orthogonalized and normalized after each iteration in order to reduce numerical error and to improve convergence.

If higher modes ($m > 6$ or so) are required, the power method becomes inefficient and one should use a different approach; this problem has not been explored in this study. One should keep in mind, however, the fact that this approach is efficient for finding the six lowest axial modes for each value of n. Referring to the frequency spectrum shown in Fig. 3, for $\ell/a = 2$, the first ninety frequencies, when arranged in numerical order, all have modes with fewer than seven axial waves. Thus the finite difference approach taken here certainly will efficiently cover a broad range of the frequency spectrum.

Energy Approach

There are a number of closely-related techniques (e.g., Rayleigh method, Rayleigh-Ritz method) which rely basically on a minimization of the difference of kinetic and potential energy. One assumes one or more deflected shapes (having undetermined amplitude) which satisfy part or all of the boundary conditions, and by making use of the strain-displacement relationships, the kinetic and strain energy expressions can be written down. Minimization of the difference of the kinetic and potential energy ultimately determines all but one of the amplitudes of the assumed deflected shapes. One of the primary advantages of this approach is that with only a one-term approximation to the mode shape, one can develop an accurate algebraic expression for the natural frequency. This has a considerable advantage when one wishes to study the frequency spectrum for a wide range of parameters. The energy approach has the disadvantage that one must assume a mode shape which satisfies at least the geometric boundary conditions; this is not always easy to do successfully for complex structures such as shells. Arnold and Warburton [8] have successfully applied the energy approach to a fixed-ended shell (i.e. all displacement quantities zero at the ends) and have obtained excellent results for the frequency. They used as an assumed mode shape

$$\begin{aligned} u &= A\,(\cos \mu x - \beta \cosh \mu x) \cos n\varphi \cos \omega t \\ v &= B\,(\sin \mu x - \beta \sinh \mu x) \sin n\varphi \cos \omega t \\ w &= C\,(\sin \mu x - \beta \sinh \mu x) \cos n\varphi \cos \omega t \end{aligned} \qquad (8)$$

where the values of μ satisfy the equation

$$\tan \frac{\mu \ell}{2a} = \tanh \frac{\mu \ell}{2a} \quad ,$$

the parameter β is defined as

$$\beta = \sin \frac{\mu \ell}{2a} \Big/ \sinh \frac{\mu \ell}{2a} \quad ,$$

and x is limited to the range

$$- \ell/2a \leq x \leq + \ell/2a \quad .$$

Similar forms hold for the even mode shapes. Because this solution agrees well with test results, and because it is widely known as an excellent solution to the problem, it has been used here as the example of approximate solutions by energy techniques.

It should be noted that the agreement of the modal forces with those from the exact solution could be improved by taking additional terms in Eq. (8) and applying the Rayleigh-Ritz technique. In the original work [8] the authors felt such refinement was unnecessary for their purposes. It should also be mentioned that Arnold and Warburton used the strain-displacement relationships as formulated by Timoshenko; these differ somewhat from those used by Flügge, but the numerical difference is not significant in the range of problems of interest here.

DISCUSSION OF RESULTS

General

Before one can compare the results of the various approaches discussed above, it is necessary to review briefly the modal behavior of cylindrical shells. For a fixed number of circumferential waves the frequency increases monotonically with an increasing number of axial half waves. This holds true for the entire range of shell parameters (a/h, ℓ/a, ν) and for all boundary conditions. The behavior is quite different when the number of circumferential waves n is varied, as indicated in Fig. 3. The value of n which corresponds to a mode shape having the minimum frequency depends strongly upon the length to radius ratio of the shell. For instance for a shell having $a/h = 500$, $\ell/a = 2$, the minimum frequency occurs with $n = 8$, $m = 1$. There are over 90 modes with values of n up to 24 and m up to 6 having natural frequencies which are less than that for the simple mode shape $n = 2$, $m = 1$. The spectrum for $n \geq 2$ is very sensitive to the bending stiffness of the shell; however, the axisymmetric mode ($n=0$) and the "beam-type" mode ($n=1$) are for all practical purposes independent of the bending stiffness (and hence independent of a/h) except for short shells ($\ell/a < 1.0$). The natural frequency for these modes is inversely proportional to a power of the axial wave length and tends toward zero as the wave length increases. For $n=0$ the natural frequencies of the shell are asympotic to the longitudinal frequencies of a bar, and, if $\ell/ma > 10$, shell frequencies can be computed with engineering accuracy using the expressions developed for a bar. For $n=1$ the natural frequencies of the shell are asymptotic to the lateral frequencies of a simple beam; if $\ell/ma > 20$, shell frequencies can be computed with engineering accuracy using simple beam formulae (one can go down to $\ell/ma \geq 8$ if the Timoshenko beam expressions are used). In order to direct our attention to the significant findings of the present study, we will in many cases examine only the frequency envelope, i.e. the lower bound to frequency spectrum for a given value of a/h, and for $m = 1$ and $n \geq 2$. The envelope

is indicated by a heavy line in Fig. 3. Although a change in the boundary conditions will alter the frequency spectrum, the general character will not be affected.

Simplified (Donnell) Equations

To evaluate the error introduced by the simplifications used in the Donnell equations, a comparison has been made between Eqs. (1) and Eqs. (2) (which include inplane inertia). For axially symmetric (n = 0) behavior the two sets of equations are essentially identical. The differences occur only in terms which have negligible influence on the numerical results. For non-axially symmetric behavior, on the other hand, there are ranges of the parameters (a/h, ℓ/a, n, m) for which there are large errors in the results as obtained from Eqs. (2). The question to be answered here is whether or not the regions of significant error coincide with regions of practical interest. The first step in answering this question is to study the asymptotic behavior of the shell for $n \geq 1$ as $\ell/ma \to \infty$. The asymptotic values for the lowest frequency for each value of $n \geq 1$ are found by omitting all axial dependence in the equations of motion; the results are independent of the boundary conditions on the shell.

$$\left(\frac{\omega}{\omega_o}\right)^2 = \Omega_e^2 = k\,\frac{n^2(n^2-1)^2}{n^2+1}, \qquad n \geq 1 \qquad \text{(Flügge Eq.)}$$

and

$$\left(\frac{\omega}{\omega_o}\right)^2 = (\delta_1\Omega_e)^2 = k\,\frac{n^6}{n^2+1}, \qquad n \geq 1 \qquad \text{(Donnell Eq.)} \qquad (9)$$

where Ω_e is the frequency ratio derived from the Flügge equations, including inplane inertia.

The error factor for the Donnell equation is δ_1 and is tabulated in Table 1. The factor δ_1 indicates the maximum error, but conclusions to be drawn from this value may be misleading. For instance, the asymptotic behavior of the Donnell equations is clearly invalid for $n = 1$; however, the Donnell equations

give excellent results for $n = 1$ over a wide range, as indicated in Fig. 4*. For $n = 2$ the error (i.e., $\delta_1 - 1.0$) in the asymptote is 33 percent. This agrees with results of previous studies, but one should note that the actual deviation encountered depends upon the length to radius ratio; as can be seen in Figs. 5 and 6, if the shell is sufficiently short, the error diminishes to zero. Although the asymptotic error is independent of the radius to thickness ratio a/h, the length of shell which can be considered sufficiently short so that the error is negligible depends upon a/h and n. Note also that although the maximum error in the asymptotes occurs for $n = 2$, the maximum error for a shell of finite length may occur in a higher circumferential mode (e.g. if $\ell/a = 20$, $a/h = 500$, the error for $n = 2$ is 3 percent, while for $n = 3$ the error is about 10 percent). For all values of n, however, the error diminishes rapidly as the number of axial waves m increases.

In order to understand the reason behind the behavior indicated in Figs. 4 to 6, it is necessary to explore briefly the source of difference between Eqs. (1) and (2). The differences between the Flügge and Donnell formulation lie basically in the expressions for the changes of curvature and twist. Flügge uses the following expressions

$$\kappa_x = \frac{w''}{a^2} \quad , \quad \kappa_\varphi = \frac{w''+w}{a^2} \quad , \quad \kappa_{x\varphi} = \frac{w'^{\cdot}}{a^2} + \frac{u^{\cdot}-v'}{2a^2} \tag{10a}$$

whereas the Donnell formulation is based on the following

$$\kappa_x = \frac{w''}{a^2} \quad , \quad \kappa_\varphi = \frac{w^{\cdot\cdot}}{a^2} \quad , \quad \kappa_{x\varphi} = \frac{w'^{\cdot}}{a^2} \tag{10b}$$

*Two curves are shown in Fig. 4, one of which is asymptotic to the simply supported beam frequency, the other is asymptotic to the fixed or clamped beam frequency. A clamped beam is developed from shell theory by requiring $u = 0$ at the boundary. The condition placed on the moment M_x has no significant influence (requiring $\partial w/\partial x = 0$ at the boundary of a simply supported shell increases the natural frequency by less than one-half percent).

The expressions for the membrane strains are identical in both theories. We can see clearly from Fig. 6 that as ℓ/a decreases, the frequency for all values of a/h approaches the membrane frequency. Since the approximations in the Donnell equations are entirely in the bending terms, it is to be expected that the error should diminish as the membrane value is approached. Moreover, it has already been noted that the frequency spectrum for $n = 1$ is essentially independent of the bending stiffness. Since the Donnell equations correctly account for the membrane strain energy, it is clear that they must accurately describe the shell behavior as long as the membrane strain energy is large compared with the bending strain energy. As the axial wave-length becomes infinite, the membrane energy goes to zero, and thus the small, but finite, bending strain energy predicted by the Donnell equations yields the finite asymptotes for the frequency, as shown in Figs. 4 and 5.

The interplay between bending and membrane strain energies is indicated schematically in Fig. 7. This sketch is based on the energy distribution as computed by Arnold and Warburton [8, 9]. The relative magnitude of the bending and membrane energies depends upon n, ℓ/a, and a/h. The relative error in the bending strain energy also depends upon these parameters.

When we compare the mode shape and modal forces we find that the Donnell equations give excellent results. The example shown in Fig. 8 illustrates this fact. Although the frequencies differ by somewhat over 2 percent, the mode shape agrees numerically to four significant figures. In order to emphasize the degree of agreement between the results of the two formulations, numerical results are presented in Table 2 for two sets of shell parameters. (The various other approximations shown in Table 2 will be discussed in the following sections.) The modal forces (which are associated with the mode shape having $w_{max} = 1.0$) agree very closely. As expected the only significant difference occurred in the moments, with a maximum deviation of 6 percent in M_φ. In all cases studied the maximum error occurred in M_φ, and the magnitude of the error is roughly equal to the factor $(\delta_1^2 - 1)$. A smaller error is observed in the axial moment M_x, as well as in the twisting moment $M_{x\varphi}$ (not shown).

It is evident that the error in the frequency as computed by Eqs. (2) arises from a difference in strain energy associated with the two formulations. This is easily demonstrated, since the mode shape, and hence all terms except the frequency in the expression for the kinetic energy, are identical in the results from both the Flügge and Donnell equations. Thus the change in frequency which has been computed must arise from a change in strain energy expressions.

Clearly the Donnell equations are an excellent approximation for predicting the dynamic behavior of cylindrical shells. Since for most practical problems we are only interested in the range ($a/h > 75$, $\ell/a < 10$), the maximum deviation to be expected in the frequency is approximately ten percent, and would occur for $n = 3$. The error diminishes when a/h or m increases, and when ℓ/a decreases. Most important of all, the Donnell equations are valid in this range for any value of $n \geq 0$, and the error diminishes from the maximum when n differs from three. When higher frequencies are considered the error diminishes rapidly to zero.

Effect of Inplane Inertia

For certain problems it is reasonable to omit the inplane inertia terms from the equations of motion. (This is not to be confused with omission of the inplane displacement components, u and v; neglecting u and v destroys the essence of the shell problem wherein the inplane displacement and normal displacement components are strongly coupled.) What we are doing, in effect, is treating the shell mass as if the mass had three components; the inplane components are put equal to zero. Since both the Flügge and Donnell equations of motion yield a cubic frequency equation, for any given nodal pattern (i.e., fixed m and n) there are three mode shapes and corresponding natural frequencies* [9]. Two of the three frequencies are, in general, an order of magnitude above the minimum of the three. The frequency spectrum shown in Fig. 3 is based on equations which

*Addition of shear deformation and rotatory inertia of the shell wall would make a total of five frequencies and mode shapes per nodal pattern; treatment of shear deformation and rotatory inertia is beyond the scope of the present paper.

include inplane inertia; however only the lower portion of the total spectrum is presented. The first, and most obvious, consequence of neglecting inplane inertia terms from the equations of motion is that the frequency equation reduces from a cubic to a first-order expression, and thus two of the three frequencies for a given nodal pattern are no longer present. The mode which is retained is the one which is associated primarily with radial motion.

The effect of inplane inertia on the remaining frequency can be studied from various points of view. A study of the asymptotic behavior of a cylindrical shell as $\ell/ma \to \infty$ reveals clearly the character of the influence of inplane inertia terms. A study of the kinetic energy of the shell gives further insight into the relationship between frequency and inplane inertia. It is of course necessary ultimately to examine the entire frequency spectrum in order to get a complete picture. Results of all three of the above approaches will be discussed in detail below.

The effect of inplane inertia on the minimum frequency of a long cylinder becomes readily apparent by comparing the asymptotic expressions given below. The parameter ρ_o is used to indicate the presence ($\rho_o = \rho$) or absence ($\rho_o = 0$) of inplane inertia. The asymptotic expressions given in Eq. (9) actually predict only the limiting values for $n = 0$ and $n = 1$. To gain a better understanding of the influence of inplane inertia on the $n = 0$ and $n = 1$ modes, it is necessary to study the asymptotic behavior of these modes separately. Only for these two cases do the boundary conditions have any influence on the asymptote. Moreover changes in the boundary conditions will only alter the magnitude of the frequency by a constant factor as $\ell/a \to \infty$, and hence for present purposes it is sufficient to examine one set of boundary conditions.

- $n = 0$, symmetric end conditions with $u = 0$ at $x = 0, \ell/a$; the asymptote for $\rho_o = \rho$ is the frequency of longitudinal vibration of a bar ($v = w = 0$), while for $\rho_o = 0$ the asymptote is the lowest extensional frequency of a ring in plane strain ($u = v = 0$):

$$
\begin{aligned}
(\omega/\omega_o)^2 &= m^2\pi^2(a/\ell)^2 && \text{, Flügge and Donnell Eqs., } \rho_o = \rho \\
&= 1 + k && \text{, Flügge Eq., } \rho_o = 0 \\
&= 1 && \text{, Donnell Eq., } \rho_o = 0
\end{aligned}
\qquad \text{(11a)}
$$

- $n = 1$, simple support at $x = 0$, ℓ/a ; asymptote for Flügge Eqs. is the frequency of lateral vibrations of a beam:

$$(\omega/\omega_o)^2 = \Omega_e^2 = (\pi^4/2)(1-\nu^2)(a/\ell)^4 \text{ , Flügge Eq., } \rho_o = \rho$$

$$= (\delta_2\Omega_e)^2 = 2(\pi^4/2)(1-\nu^2)(a/\ell)^4 \text{ , Flügge Eq., } \rho_o = 0$$

$$= (\delta_3\Omega_e)^2 = k \text{ , Donnell Eq., } \rho_o = 0 \qquad (11b)$$

- $n \geq 2$, all end conditions; asymptote for all equations is the frequency for inplane flexural vibrations of a ring in plane strain:

$$(\omega/\omega_o)^2 = \Omega_e^2 = k\, n^2(n^2-1)^2/(n^2+1) \text{ , Flügge Eqs., } \rho_o = \rho \qquad (12a)$$

$$= (\delta_2\Omega_e)^2 = k\,(n^2-1)^2 \text{ , Flügge Eqs., } \rho_o = 0 \qquad (12b)$$

$$= (\delta_3\Omega_e)^2 = k\, n^4 \text{ , Donnell Eqs., } \rho_o = 0 \qquad (12c)$$

The mode shape is essentially the same for both equation systems with and without inplane inertia, except when $n = 0$. The amplitude ratios for the asymptotic behavior when $n \geq 1$ are indicated below:

$$\bar{v}_{max} / \bar{w}_{max} = -\left(\frac{n}{n^2-(\rho_o/\rho)(\omega/\omega_o)^2}\right) \approx -\frac{1}{n} \quad , \quad u = 0 \qquad (12d)$$

The omission of the frequency ratio in the denominator of Eq. (12d) leads to negligible error in the amplitude ratio. The error incurred in omitting the inplane inertia terms is indicated by the factors δ_2 and δ_3 which are given in Table 1.

Examination of the above asymptotic expressions shows that for small values of n the inplane inertia terms have a significant influence on the frequency. Before discussing the implications of this in terms of the effect on the overall frequency spectrum for finite length shells, we will consider the effect of the various inertia terms on the kinetic energy.

Omission of inplane inertia reduces the generalized mass of the shell and hence affects the expression for the kinetic energy of the system. The error in the

frequency arises primarily from this source. The expression for the kinetic energy is

$$T = \frac{1}{2} \int_0^{2\pi} \int_0^{\ell} \int_{-h/2}^{h/2} \left[\rho_o \left(\frac{\partial u}{\partial t}\right)^2 + \rho_o \left(\frac{\partial v}{\partial t}\right)^2 + \rho \left(\frac{\partial w}{\partial t}\right)^2 \right] dz\, dx\, a d\varphi \qquad (13)$$

where $\rho_o = \rho$, if inplane inertia is included

$\rho_o = 0$, if inplane inertia is neglected

It has been shown [1] that for a very long shell the boundary conditions have no influence on the mode shape or frequency if $n \geq 2$. Thus when studying the asymptotic behavior there is no essential loss in generality in assuming that the shell is simply supported, i.e.

$$w = \bar{w}_{max} \sin \frac{m\pi x}{\ell} \cos n\theta\, e^{i\omega t} \qquad (14)$$

with similar forms for u and v . Substitution of such expressions into Eq. (13) leads to

$$T = \omega^2 \frac{m_T}{8} \left[\frac{\rho_o}{\rho} (\bar{u}_{max})^2 + \frac{\rho_o}{\rho} (\bar{v}_{max})^2 + (\bar{w}_{max})^2 \right] \qquad (15)$$

where $m_T = \rho 2\pi a \ell h$. Making use of Eq. (12d), and including inplane inertia ($\rho_o = \rho$):

$$T_e = \omega_e^2 \frac{m_T}{8} \bar{w}_{max}^2 \left[\frac{1}{n^2} + 1 \right] \qquad (16)$$

where the subscript e indicates that inplane inertia has been included. When radial inertia only is considered ($\rho_o = 0$), then

$$T_a = \omega_a^2 \frac{m_T}{8} \bar{w}_{max}^2 \qquad (17)$$

where the subscript a indicates that only radial inertia has been included. Now comparing the two formulations, for the same amplitude $\bar{w}_{max}$ and the same total mass of the shell m_T :

$$\frac{T_e}{T_a} = \frac{\omega_e^2}{\omega_a^2} \frac{n^2+1}{n^2}$$

The asymptotic expressions derived from the Flügge equations for frequency with and without inplane inertia are given in Eqs. (12a) and (12b). Substitution of these expressions into Eq. (18) shows that for the asymptotic behavior, $T_e = T_a$. The same result ($T_e = T_a$) is obtained if we use the Donnell formulation (Eqs. (9) and (12c)). (Note, however, that the asymptotic value of the kinetic energy as derived from the Donnell equations is δ_1^2 times the kinetic energy computed from results of the Flügge equations.) The conclusion that $T_e = T_a$ for the asymptotic behavior of the shell is of considerable significance in that it requires the strain energy in the two systems be identical. Therefore the mode shape and internal force distribution must be identical. By examining the numerical results for the frequency one finds that the maximum error (δ_2-1) is never much greater than its asymptotic value. Thus one expects that the forces and mode shapes will be quite close over a wide range of finite-length shells. That this is indeed the case is borne out by the data presented in Figs. 9 and 10 and in Table 2.

The mode shapes and modal forces are plotted for two cases, ($a/h = 20$, $\ell/a = 2$, $n = 3$) and ($a/h = 20$, $\ell/a = 10$, $n = 2$). In neither case can one see the difference in mode shape for any of the approximations discussed thus far. Tabular values are given in Table 2 which show that only for a short, thick shell ($\ell/a = 2$, $a/h = 20$) is there a measurable (3 percent) deviation in any of the components of the mode shape. It is interesting to observe in Figs. 9 and 10 that the deviation in results due to omission of inplane inertia is measurable only in the hoop, and, to a lesser extent, axial forces. As indicated previously, the error in the Donnell results arises primarily in the moments M_φ and, to a lesser degree, M_x.

Let us now consider the effect of the inplane inertia terms on the frequency spectrum. This can best be done in three parts: (1) consideration of the frequency spectrum for $n = 0$ and $n = 1$, (2) discussion of the frequency envelope (i.e., various values of n) for a fixed number of axial half-waves ($m = 1$), and (3) discussion of the behavior for one case with fixed n and several values of m.

Let us discuss first the behavior for $n = 0$ and $n = 1$. As noted earlier, the omission of inplane inertia reduces the frequency from a cubic to a first order equation, and hence two frequencies per nodal pattern are discarded. This is rather dramatically displayed in Fig. 11 for the axisymmetric modes ($n = 0$). In this instance all three frequencies are definitely of interest, and in fact, the minimum frequency is omitted in a portion of the spectrum when inplane inertia is neglected. For all non-zero values of n, however, the minimum frequency is retained when inplane inertia is neglected in the equations of motion.

The influence of the inplane inertia on the frequency spectrum for $n = 1$ is indicated in Fig. 12. For the sake of clarity, only one boundary condition is depicted, but the effect for other support conditions is identical. Contrary to the effect of the approximations used in the Donnell equations, the error introduced by neglecting inplane inertia does not diminish as ℓ/a decreases until comparatively small values of ℓ/a are reached. In fact for a simply supported shell, the deviation (defined as $\delta_j - 1$) increases from the asymptotic value (41 percent) to a maximum of about 45 percent in mid-range (ω/ω_o halfway between asymptotic value and 1.0) and then gradually diminishes to zero. For the shell with fixed ends the behavior is the same, except that the maximum deviation is under 43 percent.

At first glance it seems peculiar that when the inplane inertia terms are omitted, the shell frequencies for $n = 1$ are no longer asymptotic to those of the beam, even though the beam equations consider only lateral inertia terms. This apparent anomaly is easily explained when one recalls that, for $n = 1$, $\bar{v}_{max} = -\bar{w}_{max}$. This implies that the shell cross-section translates without distortion. However w depends on $\cos n\theta$ and hence has two nodes at $\theta = \pm\pi/2$; mass located on these nodal lines contributes nothing to the dynamic behavior if radial inertia only is accounted for. In fact one can show that only half of the mass of the shell is included when only radial inertia of the shell is considered. The error factor δ_2 is exactly equal to the square root of two, which is the change in frequency one obtains when the mass of the beam is divided by two.

Consider next the influence of the inplane inertia terms for $n \geq 2$. In Figs. 13 through 15, a comparison is given of the frequency envelopes as computed first with and then without inplane inertia. These figures also indicate the difference in results as obtained from the Flügge and Donnell formulations. The error introduced by the Donnell formulation (discussed in the previous section) is here essentially multiplied by the error resulting from omitting the inplane inertia terms from the Flügge equations. These figures have been computed for three different sets of boundary conditions; by comparing them, one can see that changing the boundary conditions has no noticeable influence on the magnitude of the error for any given value of n. Changing the boundary conditions may change the value of n at which the minimum frequency occurs, and hence, for a given value of ℓ/a may actually alter the error in the minimum frequency.

The behavior for a fixed value of n, but with various m, will be considered next. Figure 16 presents the frequency spectrum for a sample case $a/h = 100$ and $n = 2$, with the shell having fixed ends. This figure serves to emphasize the fact that the error does not diminish as the length decreases, and does not diminish as the number of axial half-waves m increases until the frequency ratio ω/ω_o approaches one. Similar curves could be drawn for any support conditions and any a/h. Curves for higher values of n have similar appearance, but of course the error would be smaller. By observation of numerical examples, the maximum value of the error ranges from 10 to 15 percent more than the error in the asymptotic value. The peak value obtained varied slightly with a/h, n, and the boundary conditions.

In omitting inplane inertia we have, in effect, reduced the generalized mass of the system. The magnitude of the resulting error in the frequency is relatively constant for a given value of n, but diminishes rapidly as n increases. Unlike the error due to the Donnell approximations, this error is propagated throughout the frequency spectrum with no significant attenuation in the higher axial modes. The primary effect here is a change in the frequency, with little change in the mode shape or modal forces. The frequency spectrums for $n = 0$ and $n = 1$ clearly have unacceptably large errors. When considering the error

involved in the frequency, it is well to remember that usually the square of the frequency is used in computations, and hence the errors indicated in Table 1 are magnified. For modes having a large number of circumferential waves, however, the omissions of inplane inertia terms is certainly a valid approximation.

Finite Difference Solution

In the present study the partial differential equations of motion, Eqs. (1), including inplane inertia, are reduced to a set of ordinary differential equations by assuming sinusoidal variation in the circumferential direction, as in Eq. (6). The resulting ordinary differential equations are then replaced by a set of difference equations and the differences are defined in terms of the displacements of a set of equally spaced grid points (or stations) in the axial direction. For comparison purposes, only equal spacing of grid points has been considered here. The matrix eigenvalue problem is then formulated and the solution is obtained by iterating the matrix until the eigenvalue converges to a specified number of significant figures (here taken as seven). This represents the best estimate of the eigenfrequency and eigenvector for a given number of stations. With a sufficiently large number of stations, one can, in theory, compute the actual eigenvalue exactly. In practice one is soon overwhelmed by numerical inaccuracies, or one runs out of storage capacity on the computer. However by increasing the number of stations in a series of steps, and computing an eigenvalue at each step, one can estimate with reasonable accuracy how close the result is to the correct eigenvalue.

Four sets of grids having ten, twenty, fifty, and one hundred equally spaced points have been used to generate the data for this investigation. Four sets of boundary conditions are also considered:

- Fixed ends:

$$w = v = u = \partial w/\partial x = 0 \qquad \text{at} \quad x = 0 \,, \quad \ell/a \tag{19a}$$

- Simple Support with axial restraint:

$$w = v = u = M_x = 0 \qquad \text{at} \quad x = 0, \ \ell/a \tag{19b}$$

- Clamped without axial restraint:

$$w = v = N_x = \partial w/\partial x = 0 \qquad \text{at} \quad x = 0, \ \ell/a \tag{19c}$$

- Simple support

$$x = v = N_x = M_x = 0 \qquad \text{at} \quad x = 0, \ \ell/a \tag{19d}$$

The first example (Fig. 17) is a problem in which the internal forces are well behaved (i.e. vary slowly) throughout the shell, including the boundary region. With a grid having only ten points, the eigenvalue for a shell with fixed ends is less than eight percent above the exact value*. (In the examples given here, the exact value is approached from above; however, it is equally possible for the eigenvalue to be approached from below.) With twenty points the eigenvalue is within two percent of the exact value. Not only the mode shapes, but also the internal stress resultants are accurately determined. The high peaks in the stress resultants which occur at the boundary are the only quantities which are not accurately predicted. This can be of considerable concern, of course, if one is interested in the stresses at the boundary. Although the overall mode shape and internal stress distribution are predicted with reasonable accuracy by a grid with only ten points, the peak stresses at the boundary are not adequately represented; even when 100 grid points are used, the boundary moments are less than 90 percent of the exact value. It is interesting to note that for a shorter shell ($a/h = 20$, $\ell/a = 2$), the finite difference scheme gives much better representation of these peaks at the boundaries, as shown in Table 2. With a 50-point grid the boundary value is 98 percent of the exact value. Note also that the frequency for a 20-point grid is only 0.4 percent below the exact eigenvalue. The extremely good convergence here is mainly due to the fact that the shell is short and thick enough so the boundary effects propagate throughout the shell, and the resulting stress distributions are free from regions of rapid variation.

*The exact solution is taken to mean the results from the exact solution of Eqs. (1), with inplane inertia included.

In the example shown in Fig. 17, the shell is comparatively thick (a/h = 20) and thus the effects of clamping ($\partial w/\partial x = 0$) on the moments and the effect of axial restraint ($u = 0$) on the hoop force are propagated a significant distance into the interior of the shell. In the second example (Fig. 18) the shell is much thinner (a/h = 500), but has the same length to radius ratio ($\ell/a = 10$). The value of n was arbitrarily chosen to be that for the mode having minimum frequency; hence, in the first example $n = 2$ and in the second, $n = 4$ (see Fig. 12). In the second example the effect of axial restraint on N_φ and the effects of clamping on M_x and M_φ are highly localized at the boundary. This localization causes a rather unexpected behavior in the finite difference solution. The results for mode shape and modal forces in Fig. 18 are certainly as accurate as those obtained with 10, 20, or 50 points in Fig. 17. Yet the frequency as predicted by the ten-point scheme is almost 40 percent above the exact eigenvalue, and the eigenvalue for the 20-point scheme is 11 percent too high. One normally expects to obtain a good eigenvalue even with a rather poor eigenvector. Just the contrary is found here; one obtains a good eigenvector but a poor eigenvalue. This is highly unsatisfactory because it implies that one must take considerable care in representing the boundary behavior. Not only must the mode shape be well represented (for the same maximum radial displacement, the mode shape converged to within three percent of the exact value in u and with 0.1 percent of the exact value in v after 20 points were taken) but one must also take care to have enough points to adequately represent the internal force distribution, in particular the membrane forces, N_x and N_φ and $N_{x\varphi}$.

Several additional examples were pursued in order to study this problem in more depth. Consider the results for a higher axial mode shown in Fig. 19. First, the representation of the mode shape and internal stress resultants with the 10 and 20 point schemes is not as good as it was for the lowest mode; yet the error in the eigenvalue has not changed significantly. Second, the slow convergence of the eigenvalue with increasing number of stations is not due to an inadequate representation of the shell behavior in the interior region (away from the boundaries). This can be seen by comparing Figs. 18 and 19. In the lowest mode (Fig. 18) the eigenvalue was 40 percent too high when 10 points

were used in a single axial half wave-length. For the third mode (Fig. 19) the 20-point scheme has seven points in a half-wave, but the discrepancy in the frequency is only 14 percent; the fifty point scheme has seventeen points in a half-wave, and the discrepancy in the eigenvalue is less than three percent--compared with the 11 percent discrepancy for the 20-point scheme in Fig. 18. These items illustrate the fact that the slow convergence to the exact frequency here (as compared with results shown in Fig. 17) is due partly to difficulty at the boundaries. The slow convergence to the exact eigenvalue arises from poor representation of the hoop force at the boundary. It has been shown [1] that clamping has no significant influence on the frequency for $a/h = 500$, $\ell/a = 10$. Thus the mismatch in representing the behavior of the moments at the boundary cannot have any measurable influence on the convergence of the finite difference formulation. By changing the boundary conditions from the fixed end condition ($u = v = w = \partial w/\partial x = 0$) to the condition of simple support with axial restraint ($u = v = w = M_x = 0$), one finds that the exact frequency is not significantly altered (less than one-tenth of a percent). The variation in the moments is now quite smooth near the boundaries; however the sharp spike in the hoop force is still present. As can be seen from Table 3, this change in boundary conditions does not alter the rate of convergence for finding the eigenfrequency. If we consider, instead, a clamped shell without axial restraint ($N_x = v = w = \partial w/\partial x = 0$) we find that the exact frequency is close to that for a simply supported shell. The hoop force N_φ still has a sharp spike at the boundary, but the magnitude of N_φ (which was already very small compared to N_x) has decreased by a factor of 30; the moments still have sharp spikes at the boundaries for this set of boundary conditions. The elimination of axial restraint improves the accuracy of the finite difference scheme.

The above discussion considered only the influence of boundary conditions. There are other factors which have equally strong influence on the accuracy of the results. Even if conditions are such that all the stress resultants vary smoothly near the boundaries, as for a simply supported shell, one may still need to take a large number of points to get an accurate estimate of the frequency (as can be seen in Table 3). The mode shape and modal forces for a simply supported shell

($a/h = 500$, $\ell/a = 10$) are shown in Fig. 20. Note that again the mode shape and modal forces are accurately represented with only a few points whereas one requires considerably more points to obtain an accurate estimate of the eigenfrequency. The maximum error occurs in the hoop force N_φ , which is itself a very small quantity compared to the other membrane forces. The inability to accurately estimate the frequency with a small number of points arises from the fact that the shell is long and thin. The accuracy of the frequency estimate is, in fact, affected by several parameters: the number of circumferential waves n , and the ratios ℓ/a and a/h . No precise statement can be made as to the number of points required for a given shell to obtain a given degree of accuracy. One can say, however, that the finite difference scheme will give better results for a short, thick shell than it will for a long thin one, even if the grid spacing (in multiples of the shell thickness) is the same. For a fixed number of grid points the accuracy of the finite difference approach slowly decreases as a/h or n increases; the accuracy of the results rapidly diminish as ℓ/a is increased. Examination of the data in Table 4 will illustrate this point.

The finite difference scheme certainly is a powerful tool for investigating the dynamic behavior of structures, since it can accurately predict not only the eigenfrequencies, but the modal stress resultants as well. However, even using a large number of points, one still may not be able to accurately predict the peak stresses which arise at the boundary; a non-uniform spacing of points near the boundary will lead to faster convergence for a given number of points. Finally, all of the comments here have been based on a one-dimensional array. If one must treat the two dimensional problem, the size of the system rapidly gets out of hand. A grid with 40 points axially and 50 circumferentially is still somewhat coarse, yet one now has a 6000 by 6000 matrix to evaluate. In this type of problem, another approach--such as finite element--may yield a simpler scheme.

Energy Method

As noted earlier the work of Arnold and Warburton [8] is used as an example of the energy method. The objective of their paper was to develop a solution which would predict the natural frequencies of a cylindrical shell with fixed ends (all displacement quantities zero at the boundaries). They used an energy approach which required the use of an assumed displacement function. As in all the solutions discussed herein, they assumed sinusoidal variation in the circumferential direction for the displacement quantities (this does not impose any limitation on the generality of the solution for a complete shell). The form of the displacement function for the modal behavior of a clamped beam was used to approximate the axial variation of u, v, w . The kinetic and strain energy were then written in terms of the displacements based on the strain-displacement relation developed by Timoshenko. Application of the Lagrange equations yielded three simultaneous algebraic equations in four unknowns, A , B , C , and ω (these symbols are defined by Eq. 8).

The solution of Arnold and Warburton gives an excellent representation of the frequency spectrum, as indicated in Fig. 21. The maximum error in the frequency envelope is on the order of three percent* and is essentially independent of a/h and independent of n . The error for a constant value of n increases as ℓ/a decreases, and may reach a maximum of about ten percent for m = 1 (Fig. 22). However the error rapidly diminishes as the number of axial waves increases, as can be seen in Fig. 22. Unlike the solution of the Donnell equations, the Arnold and Warburton results accurately represent the asymptotic behavior as $\ell/ma \to \infty$, but are in error in the representation for small values of ℓ/ma where the membrane behavior is predominant. As the number of axial waves increases, the Arnold and Warburton approximation gets better. This is to be expected since it is known [1] that as the number of axial waves increases the behavior for any support condition approaches the behavior for a simply supported shell. As the shell becomes longer or as m increases, the importance of the hyperbolic

*Arnold and Warburton's results are here compared with the exact solution, where the exact results are obtained from the solution of the Flügge equations with inplane inertia.

functions in Eq. (8) rapidly diminishes; the behavior is then governed by the sinusoidal terms which in themselves will represent exactly the simple support behavior if in Eq. (8) $\mu = m\pi\, a/\ell$. It has been shown by Arnold and Warburton [8] that the roots for μ are given by $\mu = (2m-1)\pi\, a/2\ell$ for $m = 2, 3, 4, \cdots$ Thus as m increases the roots for μ decrease to the value for a simply supported shell.

As expected, the energy approach gives a better estimate for the eigenvalues than for the mode shapes and modal forces. This is contrary to the somewhat surprising findings in the finite difference examples, wherein the mode shape and modal stresses were in several instances better than the eigenvalue. When one considers the distribution of the stress resultants, one finds that the Arnold and Warburton solution represents reasonably well the forces in the interior of the shell, but the spikes at the boundaries are not even approximated. Note that, in contrast to our experience with the finite difference schemes, this inability to approximate the boundary behavior does not have a serious consequence in the computation of the frequency. These points are illustrated by the examples given below.

The mode shape and modal forces for a thin but comparatively short shell ($a/h = 500$, $\ell/a = 2$) are presented in Fig. 23; as in the previous studies, these comparisons are based on a mode shape having a unit maximum radial displacement. The error in the frequency for this case is about four percent. The error in the mode shape is about eight percent. Here the error for any given function is determined by comparing the maximum deviation at any point to the maximum amplitude of the function. As can be seen in Fig. 23 the error lies in the representation of the axial dependence of the mode shape, rather than in the relative amplitude of the u, v, w components; this observation holds true for all values of a/h and ℓ/a . The essential omission in the modal forces is in the description of the boundary behavior. Except for the hoop force N_φ , the stresses away from the boundaries are predicted with reasonable accuracy. The hoop force is grossly in error, but it is actually a small quantity when compared to N_x and hence a large error in N_φ has little over all influence.

Figure 24 presents results for a longer shell $a/h = 500$, $\ell/a = 10$, with $n = 8$. The behavior is very similar to that of the shell studied above; the errors are smaller in this instance, as expected. Figure 25 was developed for the same shell ($a/h = 500$, $\ell/a = 10$) used above, but having $n = 2$ and $m = 3$. Note in this instance that most of the error in both the forces and the mode shape is confined to the half wave nearest the boundary. The spikes in the moments M_x and M_φ are still not predicted, but the hoop force is approximated more closely than was done for the lower mode (Fig. 24).

It must be reiterated that Arnold and Warburton were seeking only a prediction of the frequency, not of the internal forces, and their solution does an excellent job of this. The energy solution developed by them gives good results for the mode shape and modal forces, as well as for the frequency. The only significant error lies in the inability to predict the edge moments, which may well be of considerable engineering interest. There are two serious drawbacks to the approach used here. First, one cannot readily handle a variety of boundary conditions. An entirely new solution must be generated for each case of interest. Second, in general one does not have an exact solution to compare with the results of an approximate analysis. Hence, even with experimental verification or comparison with results of another approximate solution, one has difficulty in establishing the magnitude of the error in the results. One can take more terms in the assumed mode shape, but if it is important to represent accurately the stress-resultants near the boundary, and if one uses smooth functions to correct the assumed mode shape, the answer may be very slow in converging to the exact solution. These disadvantages are offset by the significant advantage of being able to compute the frequency spectrum for a large number of cases with a minimum of high-speed computer time. This is discussed in more detail below. The present study would have been considerably more limited if the Arnold and Warburton results [8, 9], or something similar, had not been available.

Computer Time Required for Solution

Three methods for solving the equations of motion of a cylindrical shell have been discussed here: an exact solution, a finite difference solution, and an energy solution. Of the three only the energy approach yields an explicit expression for the frequency which can be solved by hand computation. Both the exact solution and the finite difference solution rely entirely upon a high-speed digital computer for numerical evaluation of the eigenfrequency. Comparison of mode shape and modal forces for a number of different sets of shell parameters is feasible only if a high-speed computer is used, no matter what approach is taken to get the eigenfrequency. The choice of a particular method of solution may rest upon the amount of computer time required to obtain a solution. Although the time required to compute a single eigenvalue is quite small by any of the above three approaches, often one is trying to construct a set of curves for some particular purpose and hence will run many cases through a given program.

The exact solution uses an iterative scheme requiring an initial estimate which is reasonably close to the actual value (the Arnold and Warburton solution was used to obtain such initial estimates). The computer run time depends upon how accurate the initial estimate is, and what degree of accuracy is required in the result. On the average the exact program requires seven iterations to converge to seven significant figures* in the eigenvalue (if the initial estimate is within ten percent of the actual eigenvalue), and will compute about 14 eigenvalues and corresponding eigenvectors in one minute.

The finite difference solution also uses an iterative scheme (power method) which takes about seven to ten iterations to determine eigenvalues to seven places*. The computer run time depends upon the number of points in the finite difference grid, and average times have been indicated here for various cases: for a 10-point grid, one can compute about 25 eigenvalues and related eigenvector per minute; for a 20-point grid, one can compute about 16 eigenvalues per minute; for a 50-point grid, one can compute about 7 eigenvalues per minute; for a 100-point grid,

*Seven significant figures are required in the eigenvalue for internal numerical consistancy in order to obtain a valid eigenvector. Only the first three or four figures of the eigenvalue have any practical meaning.

one can compute 4 eigenvalues per minute.

At this point it is worth returning to the question of handling large finite difference nets. As noted previously, for a long, thin shell ($a/h = 500$, $\ell/a = 10$), the convergence is poor, and one may have to take 50 points along the generator to have an acceptable solution. If the shell had asymmetric cutouts or had a concentrated mass attached at one point, one would have to use a two-dimensional grid. If the grid had only 50 points axially and 40 circumferentially, one would have a 6000 degree-of-freedom system. Of course the resulting matrix would be strongly banded about the diagonal, with non-zero elements occurring in about 100 columns on either side of the diagonal. A 6000 degree-of-freedom system has been solved for a statics problem, and the computer run time is on the order of ten minutes. (It is significant that one could obtain a solution without becoming overwhelmed by numerical errors.) It is possible that an optimized program could be written which would solve the eigenvalue for the same size matrix in about 15 minutes.

The Arnold and Warburton solution is an algebraic expression which can be evaluated directly. The program here has been used to scan the frequency spectrum and locate the five lowest eigenvalues for a given a/h and ℓ/a; considering such an operation as a single case, the program can handle about 150 cases per minute. Although no accurate check has been made, the program evaluates in excess of 2000 eigenvalues per minute. This points up one of the primary advantages of a solution of this type. The Arnold and Warburton solution has been an essential tool in making preliminary studies to determine what areas need more extensive investigation by the slower but more exact methods.

The required computer run times indicated above are based on the use of the IBM 7094. Future generations of computers with increased storage capacity and shorter times required to perform arithmetical operations will alter the magnitude of the times indicated above. The ratio between the various operations, however, will remain valid for some time to come.

CONCLUSIONS

This study has covered a number of points which can be summarized as follows:

(1) Approximations in the equations of motion:

- Simplified equations of motion
  The Donnell-type equations have had widespread usage, but have often been limited to ranges in which the number of circumferential waves n is large. The present study shows that the Donnell equations are valid for all n and all a/h if we restrict attention to shells having $\ell/ma < 20$. The error incurred in the frequency rapidly diminishes as ℓ/ma decreases. The mode shape and membrane forces N_x and N_φ are accurately determined; the error if any will occur in the moments M_x and M_φ . The boundary values of all quantities are accurately determined.

- Omission of inplane inertia
  The primary effects of neglecting inplane inertia terms are (1) the omission of two higher frequencies for each nodal pattern, and (2) the remaining frequency is increased in magnitude. The magnitude of the error in the frequency depends upon n , but is insensitive to a/h and ℓ/a . The mode shape and modal forces are not significantly affected by the omission of inplane inertia. For large values of n (say $n > 10$), there is no significant effect of inplane inertia, and it is a reasonable approximation for that range.

(2) Approximate solutions

- One dimensional finite difference solutions give good results but require a large number of points (about 50) to accurately describe the lowest mode of a long thin shell ($a/h = 500$, $\ell/a = 10$). The accuracy of the frequency estimate becomes poorer as ℓ/a , a/h , or n are increased; the results are most sensitive to changes in ℓ/a .

The eigenvector is more accurately determined than the eigenvalue; however, the finite difference scheme has difficulty representing the rapid changes at the boundary. This suggests that the ideal program would have variable spacing for grids near the boundary.

The energy method, as represented by the Arnold and Warburton solution, gives excellent results for the frequency. The modal forces are predicted with reasonable accuracy, but as with the finite difference schemes, the boundary behavior is completely in error. Unlike the finite difference approach, where a simple change in the number of stations may improve the prediction of boundary behavior, any improvement on Arnold and Warburton's solution will require an extensive amount of work. The major advantage of the energy approach--or any other which will yield an explicit expression for the frequency--is that the algebraic expressions are readily evaluated; one can do extensive exploring in a minimum time. Clearly such a solution is--or should be--a vital part of any research worker's program.

(3) Computer time required for solution

The advent of the high-speed digital computer has opened new vistas for exploration. Large scale finite difference schemes, as well as iterative techniques to find exact solutions, are possible only with the use of computers. The machine time required to generate a single solution, however, is deceptively low. The purpose of any mathematical study of the behavior of shells is ultimately to gain some insight into the physical behavior of the structure so that one can develop information of engineering interest. In problems such as the present one, this requires extensive numerical evaluation, and the computer time required to produce the data is of considerable interest. The evaluation of the explicit results provided by the energy approach is considerably faster from computational standpoint, and hence is of immense value in selecting regions to be explored in depth by more exact means.

ACKNOWLEDGMENT

This work was sponsored by the Lockheed Missiles and Space Company Independent Research program. The author would like to express his appreciation for the contribution of Mr. Perry Stern, who developed the computer program for solving the finite-difference eigenvalue problem. The author would also like to thank Miss Karen Murata for her assistance in running the computer programs to obtain the data for the figures, and Drs. Charles Coale and Ghassan Khabbaz for their constructive advice during the writing of the paper.

References

1. K. Forsberg, "Influence of boundary conditions on the modal characteristics of thin cylindrical shells, " AIAA J., vol. 2, no. 12, pp 2150-2157 (1964)
2. W. Flügge, Stresses in Shells, Springer-Verlag, Berlin, 1960, chap. 5, pp 219, 220, and 233
3. J. E. Greenspon, "Vibrations of a thick-walled cylindrical shell--comparison of the exact theory with approximate theories," J. Acoust. Soc. of Amer., vol. 32, no. 5, pp 571-578 (1960)
4. P. M. Naghdi, Foundations of elastic shell theory, T.R. 15, Univ. of Calif., Jan 1962
5. E. I. Ivaniuta and R. M. Findel'shtein, "On the influence of tangential inertial forces on the magnitude of the free-vibration frequency of a thin cylindrical shell," Issled. po Uprug. i Plastich., no. 2, pp 212-215 (1963)
6. N. J. Hoff, "The accuracy of Donnell's equations," J. Appl. Mech., vol. 22, no. 3, pp 329-334 (1955)
7. E. Bodewig, Matrix Calculus, North-Holland Publishing Company, Amsterdam, 1956, pp 230-280
8. R. N. Arnold and G. B. Warburton, "Flexural vibrations of thin cylinders," Institution of Mech. Engr. Proc., V167, pp 62-80 (1953)
9. R. N. Arnold and G. B. Warburton, "Flexural vibrations of the walls of thin cylindrical shells having freely supported ends," Proc. Roy. Soc. (London) A197, pp 238-256 (1948)

Table 1

Error in asymptotes for the minimum frequency of a cylindrical shell based on results obtained from Flügge and Donnell equations with and without inplane inertia. The error is given by $\delta_j - 1$.

n	δ_1	δ_2	δ_3
1	-	1.414	-
2	1.333	1.118	1.490
3	1.125	1.054	1.186
4	1.067	1.031	1.100
5	1.042	1.020	1.063
6	1.029	1.014	1.043
7	1.021	1.010	1.031
8	1.016	1.008	1.024
9	1.013	1.006	1.019
10	1.010	1.005	1.015

The error factor is the ratio of the frequency as computed from an approximate set of equations of motion to the frequency as computed from the Flügge equations including inplane inertia.

$\delta_1 = n^2/(n^2-1)$, error factor for Donnell Eq., inplane inertia included

$\delta_2 = (n^2+1)^{1/2}/n$, error factor for Flügge Eq., radial inertia only

$\delta_3 = \delta_1 \cdot \delta_2$, error factor for Donnell Eq., radial inertia only

Table 2

Comparison of natural frequency, modal displacement and modal force amplitudes as computed by various methods for two sets of shell parameters.

QUANTITY	METHOD OF SOLUTION						
	EXACT SOLUTION (FLÜGGE)	DONNELL (INPLANE INERTIA INCL.)	RADIAL INERTIA ONLY		FINITE DIFFERENCE		ARNOLD AND WARBURTON
			FLÜGGE	DONNELL	20 PTS.	50 PTS.	
CASE 1*							
ω/ω_o	0.01508	0.01541	0.01555	0.01589	0.01689	0.01540	0.01548
u_{max}	±0.01799	±0.01799	±0.01799	±0.01799	±0.01749	±0.01794	±0.01803
v_{max}	-0.2507	-0.2507	-0.2507	-0.2507	-0.2507	-0.2507	-0.2505
w_{max}	1	1	1	1	1	1	1
$\tilde{N}_x$ max	0.009127	0.009126	0.009130	0.009129	0.008903	0.009101	0.009424
$\tilde{N}_x$ min	-0.01504	-0.01504	-0.01504	-0.01505	-0.01398	-0.01510	-0.01649
$\tilde{N}_\varphi$ max	0.000162	0.000162	0.000162	0.000165	0.000204	0.000156	0.001000
$\tilde{N}_\varphi$ min	-0.004511	-0.004512	-0.004512	-0.004513	-0.004193	-0.004530	-0.004945
$\tilde{M}_x$ max	9.291	9.278	9.293	9.281	0.378	0.691	0.302
$\tilde{M}_x$ min	-4.676	-4.966	-4.676	-4.966	-4.674	-4.675	-4.681
$\tilde{M}_\varphi$ max	2.783	2.784	2.784	2.784	0.109	0.203	0.0961
$\tilde{M}_\varphi$ min	-15.05	-16.05	-15.05	-16.05	-15.05	-15.05	-15.05
CASE 2*							
ω/ω_o	0.3117	0.3188	0.3273	0.3345	0.3105	0.3117	0.3256
u_{max}	±0.03482	±0.03494	±0.03374	±0.03381	±0.03447	±0.03477	±0.03689
v_{max}	-0.3195	-0.3195	-0.3159	-0.3158	-0.3196	-0.3195	-0.3161
w_{max}	1	1	1	1	1	1	1
$\tilde{N}_x$ max	0.1131	0.1126	0.1131	0.1127	0.1107	0.1127	0.1190
$\tilde{N}_x$ min	-0.1545	-0.1541	-0.1506	-0.1500	-0.1362	-0.1460	-0.1702
$\tilde{N}_\varphi$ max	0.06971	0.07144	0.07956	0.08174	0.06899	0.06963	0.08088
$\tilde{N}_\varphi$ min	-0.06447	-0.06513	-0.06309	-0.06368	-0.03991	-0.04279	-0.05065
$\tilde{M}_x$ max	16.63	16.58	16.57	16.53	15.14	16.37	7.219
$\tilde{M}_x$ min	-5.471	-5.652	-5.468	-5.648	-5.438	-5.466	-6.803
$\tilde{M}_\varphi$ max	4.943	4.974	4.928	4.958	4.502	4.868	2.121
$\tilde{M}_\varphi$ min	-8.888	-9.886	-8.887	-9.885	-8.878	-8.886	-9.286

*CASE 1: $a/h = 500$, $\ell/a = 10$, $n = 4$, $m = 1$, $\nu = 0.3$
CASE 2: $a/h = 20$, $\ell/a = 2$, $n = 3$, $m = 1$, $\nu = 0.3$

Table 3

Comparison of frequencies obtained from finite difference formulation for various numbers of stations and various boundary conditions

Number of Stations	FREQUENCY RATIOS FOR VARIOUS BOUNDARY CONDITIONS					
	$w = v = 0$ $u = w' = 0$	Error (%)	$w = v = 0$ $u = M_x = 0$	Error (%)	$w = v = 0$ $N_x = M_x = 0$	Error (%)
One Axial Half Wave ($m = 1$)						
10	0.02101	39	0.02101	39	0.01232	21
20	0.01689	12	0.01689	12	0.01076	6
50	0.01540	2	0.01540	2	0.01028	1
100	0.01517	0.6	0.01517	0.7	0.01021	0.4
Exact	0.01508		0.01507		0.01017	

The above frequencies are computed for the following set of parameters:

$a/h = 500$, $\ell/a = 10$, $n = 4$, $m = 1$, $\nu = 0.3$

Table 4

Comparison of frequencies obtained from finite difference formulation for various numbers of stations and various sets of shell parameters. (Boundary conditions: $w = v = N_x = M_x = 0$ at $x = 0$, ℓ/a)

Number of Stations	FREQUENCY RATIOS FOR VARIOUS SETS OF PARAMETERS					
	$\ell/a = 2$, $n = 2$			$\ell/a = 10$, $n = 2$		
	$a/h =$ 100	$a/h =$ 500	$a/h =$ 5000	$a/h =$ 100	$a/h =$ 500	$a/h =$ 5000
10	0.3277	0.3274	0.3274	0.02520	0.02397	0.02392
20	.3275	.3272	.3272	.02282	.02146	.02140
50	.3275	.3272	.3272	.02210	.02069	.02063
100	.3274	.3272	.3272	.02200	.02058	.02052
Exact	0.3274	0.3272	0.3271	0.02195	0.02053	0.02047
	$n = 8$ $\ell/a = 2$ $a/h = 500$*		$n = 4$ $\ell/a = 2$ $a/h = 500$	$n = 4$ $\ell/a = 10$ $a/h = 500$		
10	0.08310		0.1264	0.01232		
20	0.07930		0.1243	0.01076		
50	0.07815		0.1237	0.01028		
100	0.07805		0.1237	0.01021		
Exact	0.07804		0.1236	0.01017		

*Frequency ratios are for fixed ends for this case.

LIST OF ILLUSTRATIONS

Fig No.

1 Coordinate system and shell element

2 Nodal Patterns

3 Portion of frequency spectrum for a/h = 500

4 Comparison of results from Flügge and Donnell equations for n = 1

5 Frequency envelope, comparing results of Flügge and Donnell Eqs. (including inplane inertia) for simple support.

6 Frequency spectrum for n = 2 , m = 1 and m = 7 , comparing results of Flügge and Donnell Eqs.

7 Sketch of strain energy vs. n (based on Arnold and Warburton's results)

8 Comparison of results from Flügge and Donnell eqs. (including inplane inertia) for mode shape and modal forces (a/h = 500, ℓ/a = 10)

9 Comparison of results from Flügge and Donnell Eqs. (with and without inplane inertia) for mode shape and modal forces (a/h = 20 , ℓ/a = 2)

10 Comparison of results from Flügge and Donnell Eqs. (with and without inplane inertia) for mode shape and modal forces (a/h = 20 , ℓ/a = 10)

11 Effect of inplane inertia terms on axisymmetric mode (n = 0)

12 Effect of inplane inertia terms on "beam-type" mode (n = 1)

13 Frequency envelope, comparing results of Flügge and Donnell Eqs. (with and without inplane inertia) for simple support

14 Frequency envelope, comparing results of Flügge and Donnell Eqs. (with and without inplane inertia) for fixed ends

15 Frequency envelope, comparing results of Flügge and Donnell Eqs. (with and without inplane inertia) for simple support without tangential restraint

16 Frequency spectrum for a/h = 100 , n = 2 , m ≥ 1 , indicating influence of inplane inertia terms

17 Comparison of finite difference solution with exact solution for a/h = 20 , ℓ/a = 10 , n = 2 , m = 1 ; fixed ends

18 Comparison of finite difference solution with exact solution for a/h = 500 , ℓ/a = 10 , n = 4 , m = 1 ; fixed ends

19 Comparison of finite difference solution with exact solution for a/h = 500 , ℓ/a = 10 , n = 4 , m = 3 ; fixed ends

20 Comparison of finite difference solution with exact solution for a/h = 500 , ℓ/a = 10 , n = 4 , m = 1 ; simple support

21 Frequency envelope, exact solution and Arnold and Warburton's approximate solution

22 Frequency distribution for $n = 2$, $m \geq 1$, comparing exact solution and Arnold and Warburton's approximate solution

23 Comparison of Arnold and Warburton's solution with exact results for $a/h = 500$, $\ell/a = 2$, $n = 8$, $m = 1$

24 Comparison of Arnold and Warburton's solution with exact results for $a/h = 500$, $\ell/a = 10$, $n = 4$, $m = 1$

25 Comparison of Arnold and Warburton's solution with exact results for $a/h = 500$, $\ell/a = 10$, $n = 4$, $M = 3$

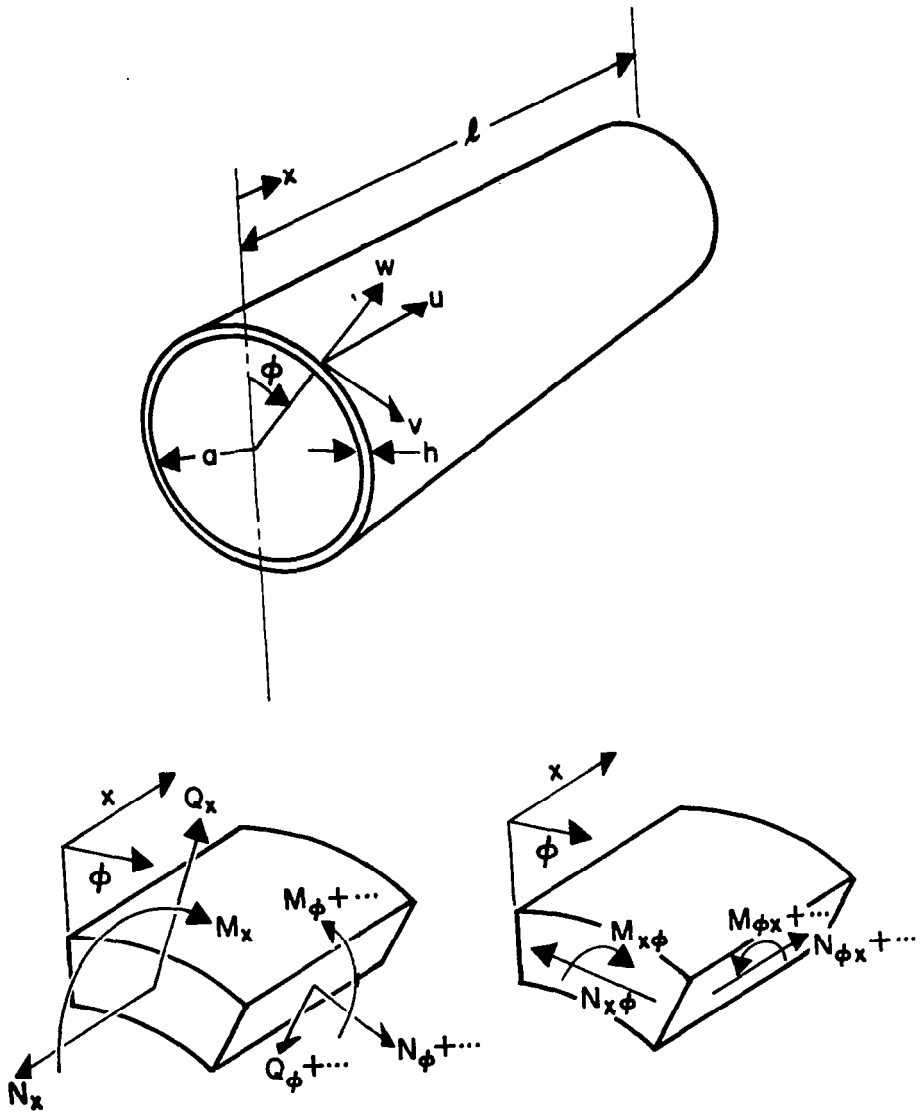

Fig. 1 Coordinate system and shell element

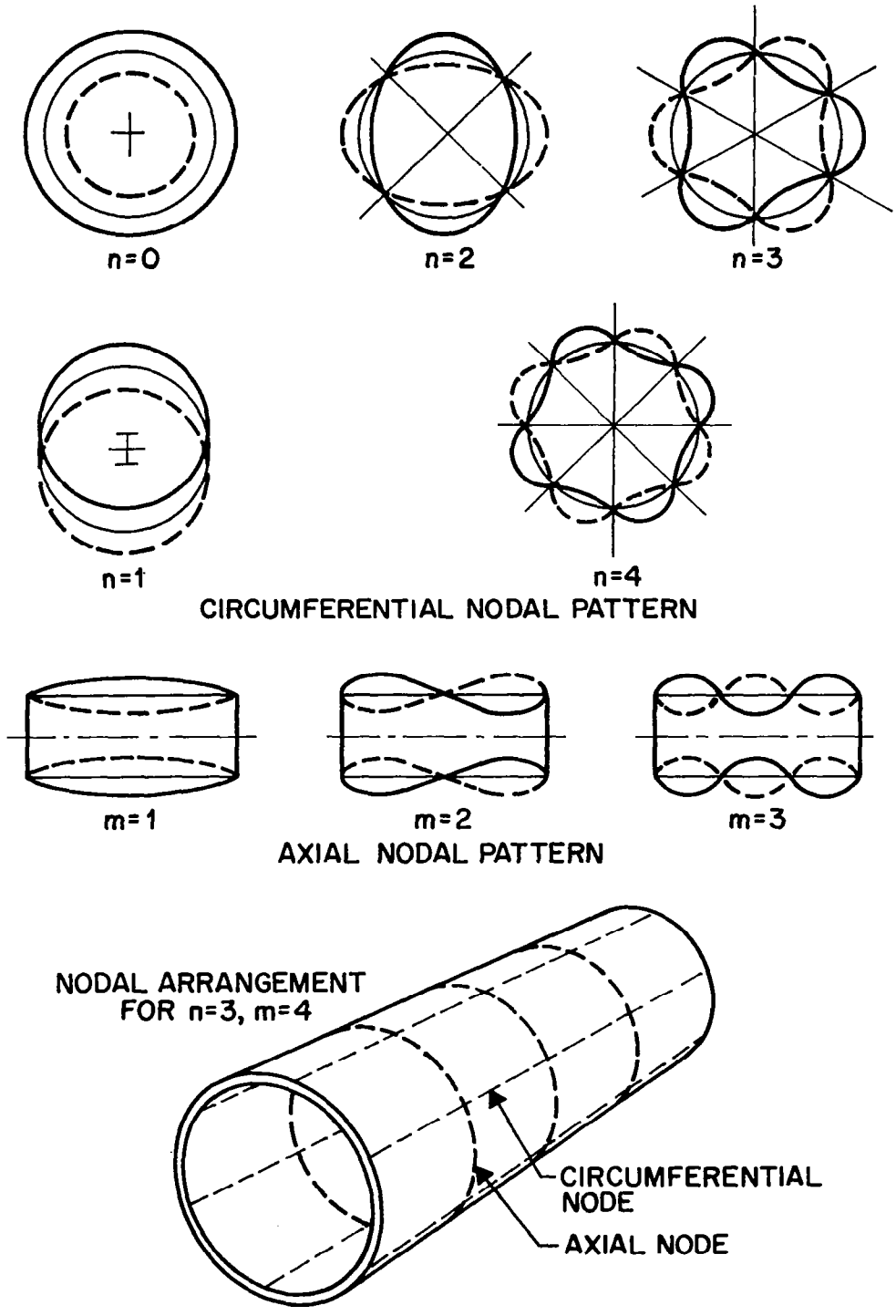

Fig. 2 Nodal Patterns

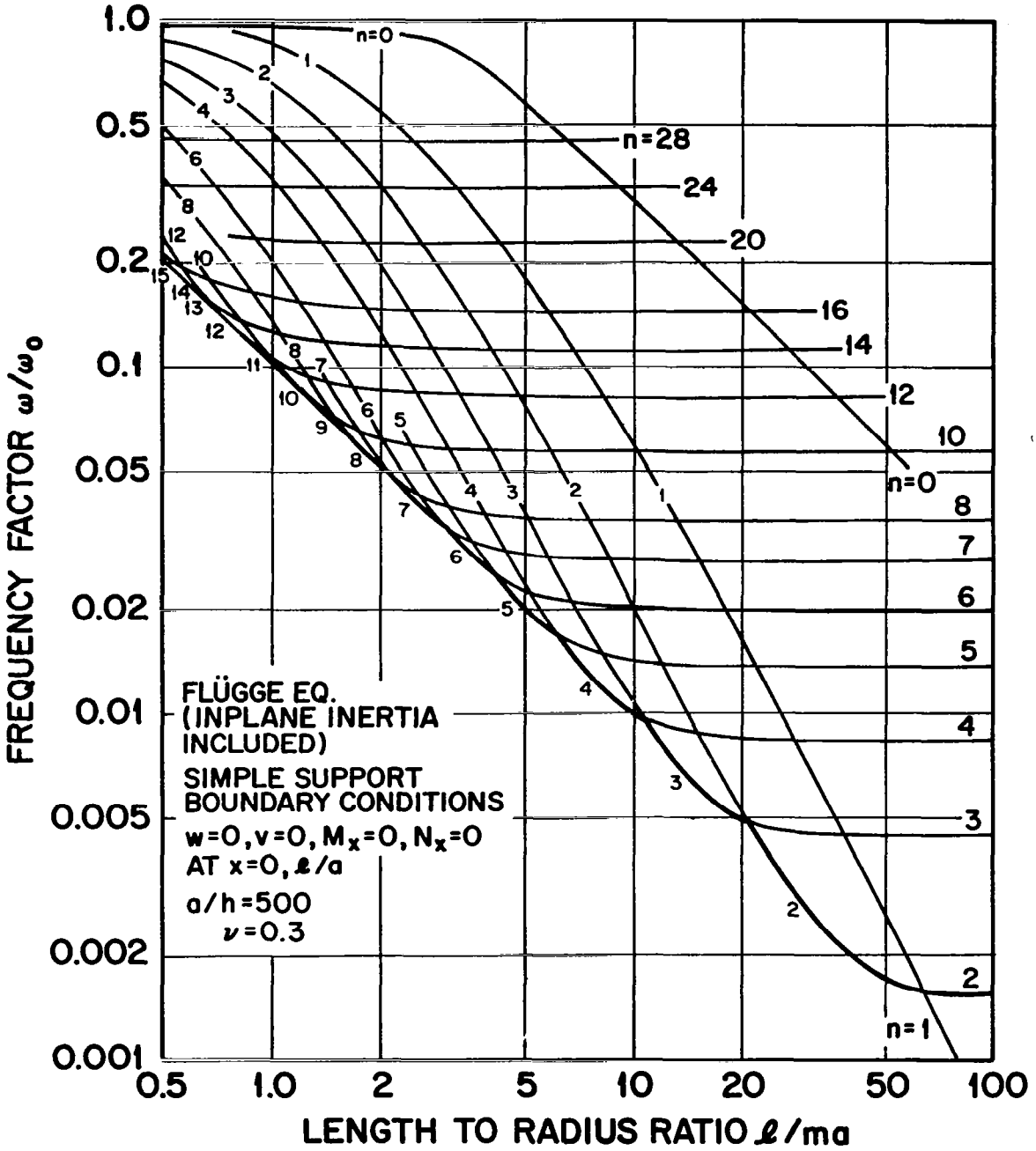

Fig. 3 Portion of frequency spectrum for a/h = 500

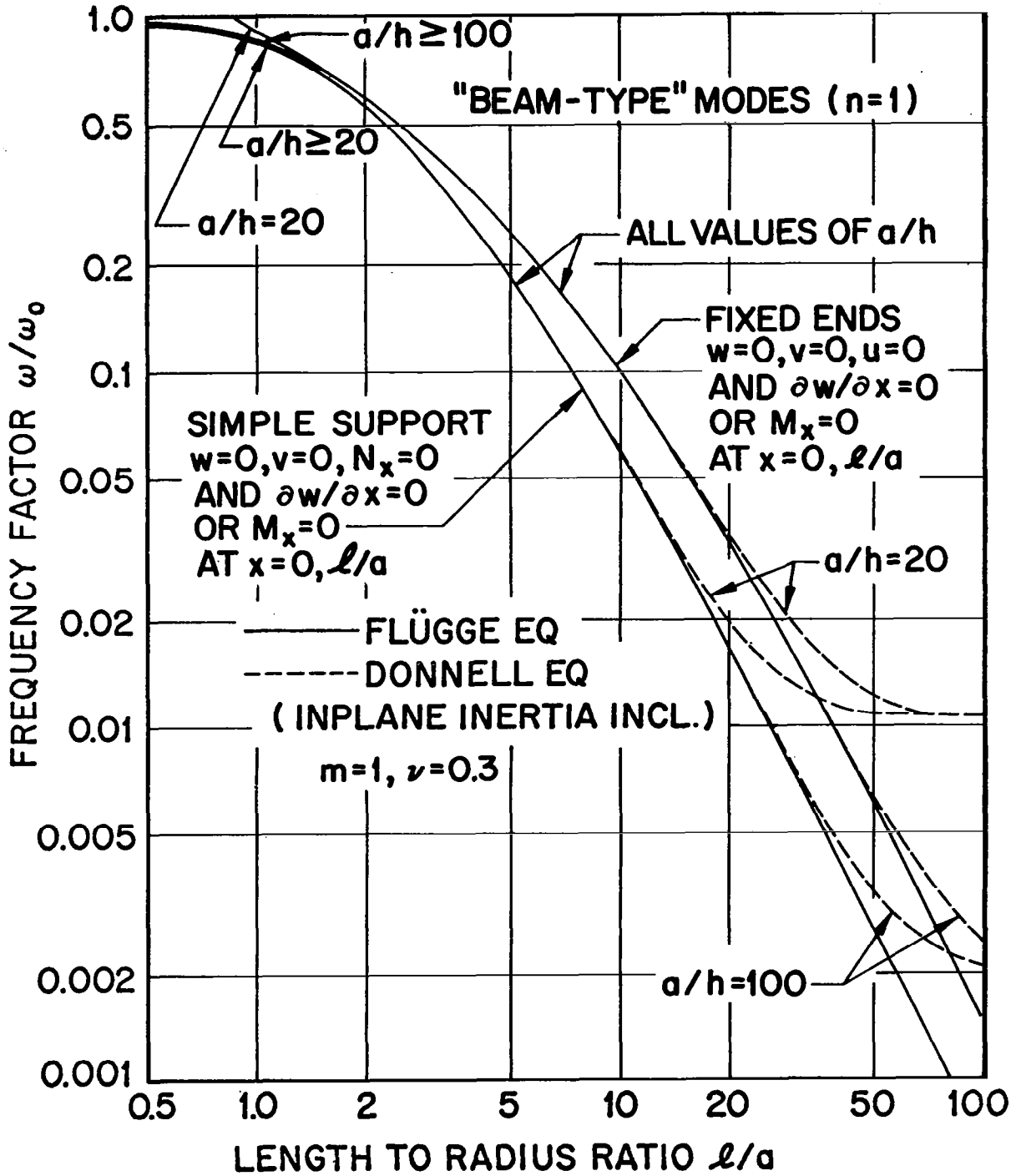

Fig. 4 Comparison of results from Flügge and Donnell equations for n = 1

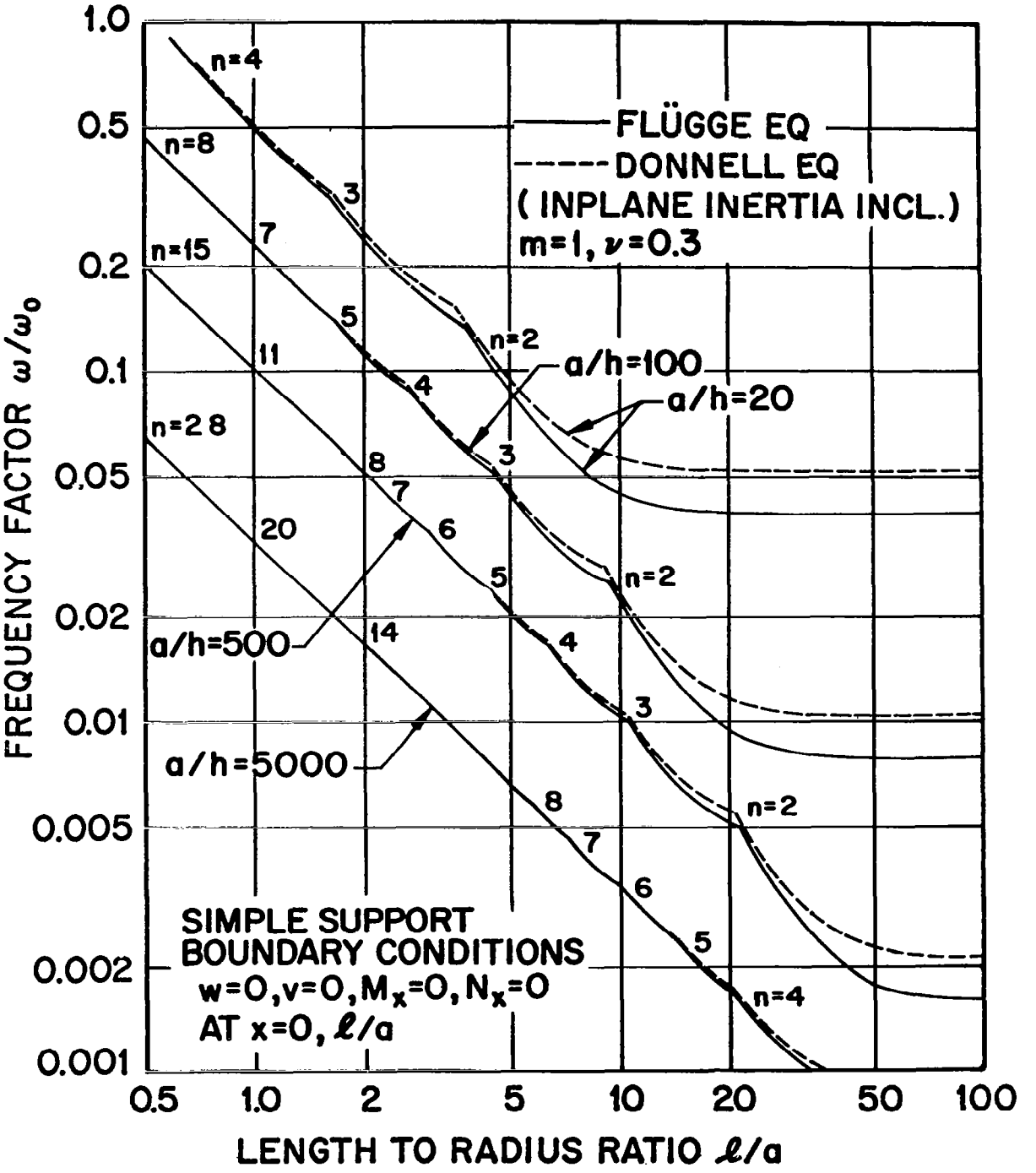

Fig. 5 Frequency envelope, comparing results of Flügge and Donnell Eqs. (including inplane inertia) for simple support

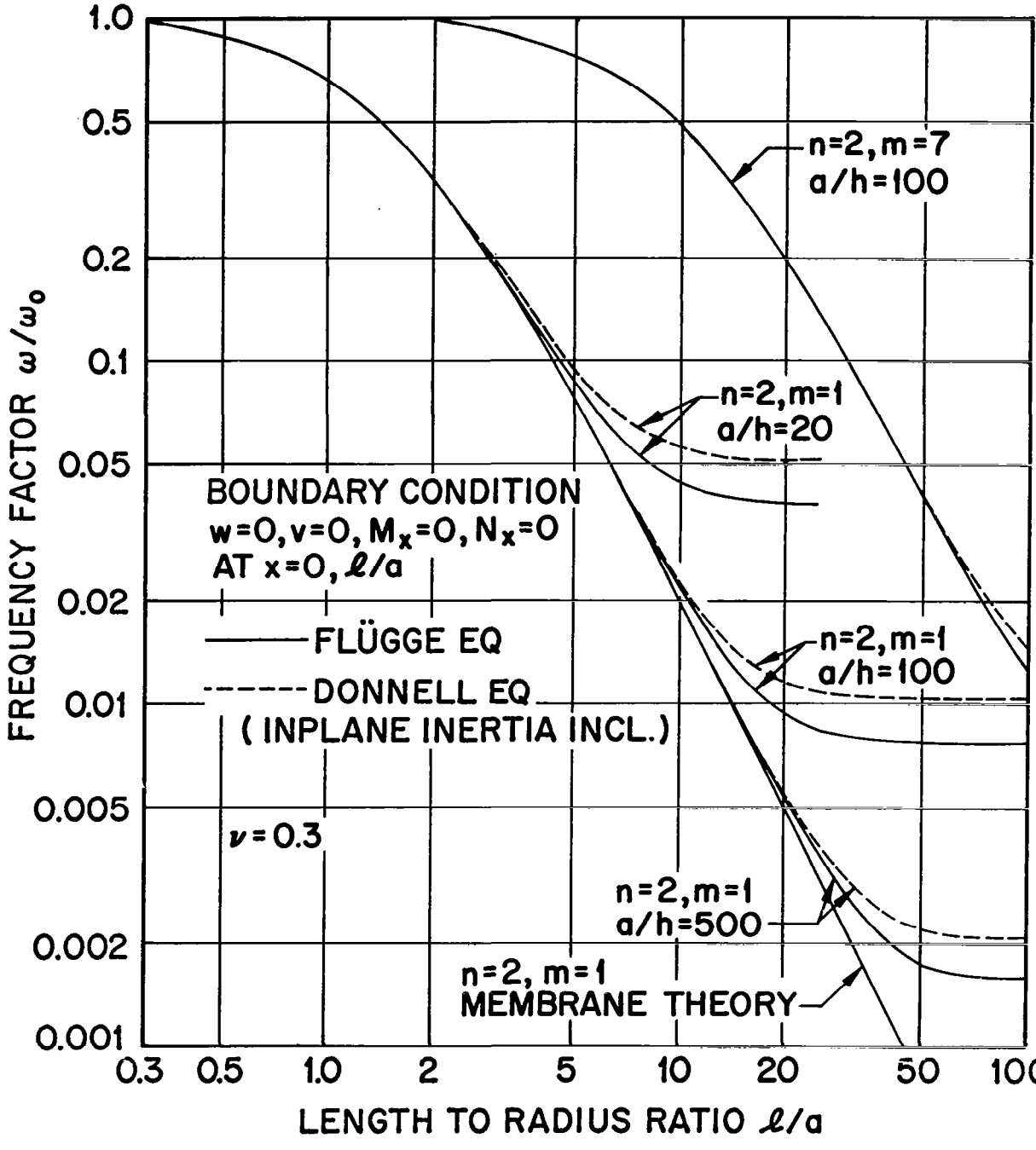

Fig. 6 Frequency spectrum for n = 2, m = 1 and m = 7, comparing results of Flügge and Donnell Eqs.

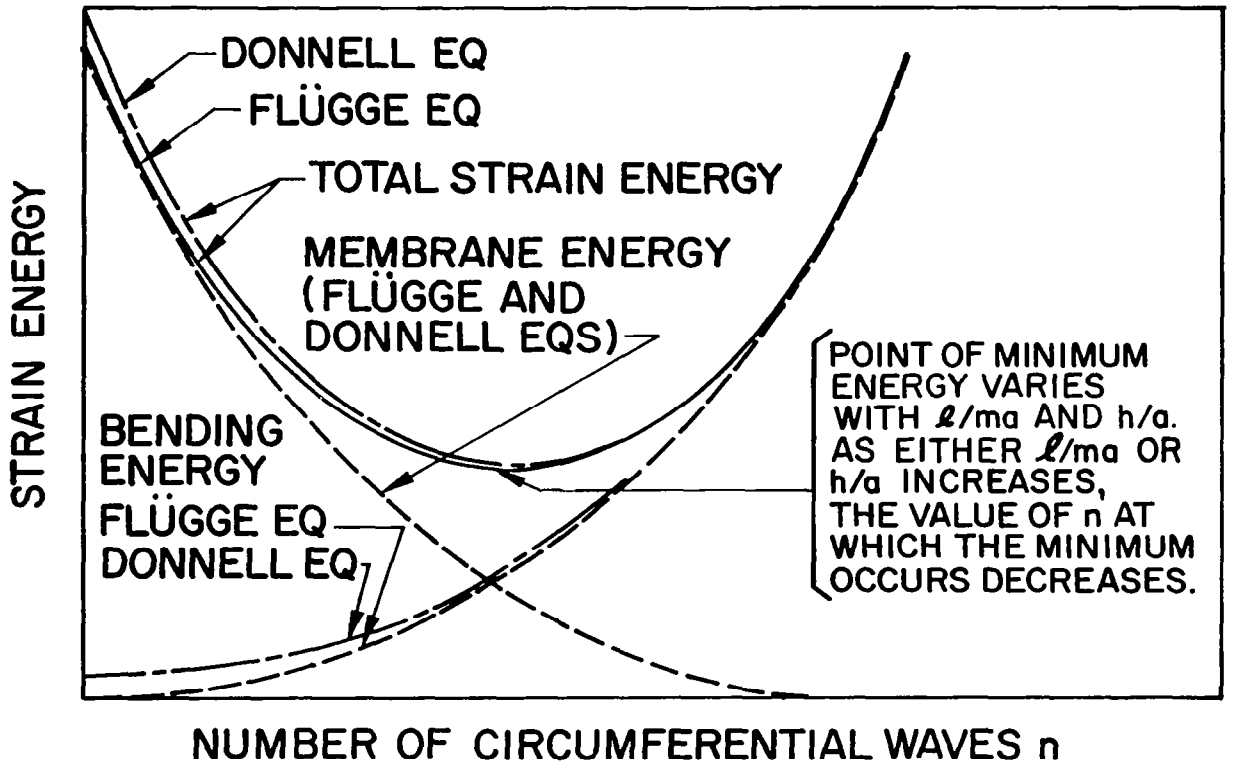

Fig. 7 Sketch of strain energy vs. n (based on Arnold and Warburton's results)

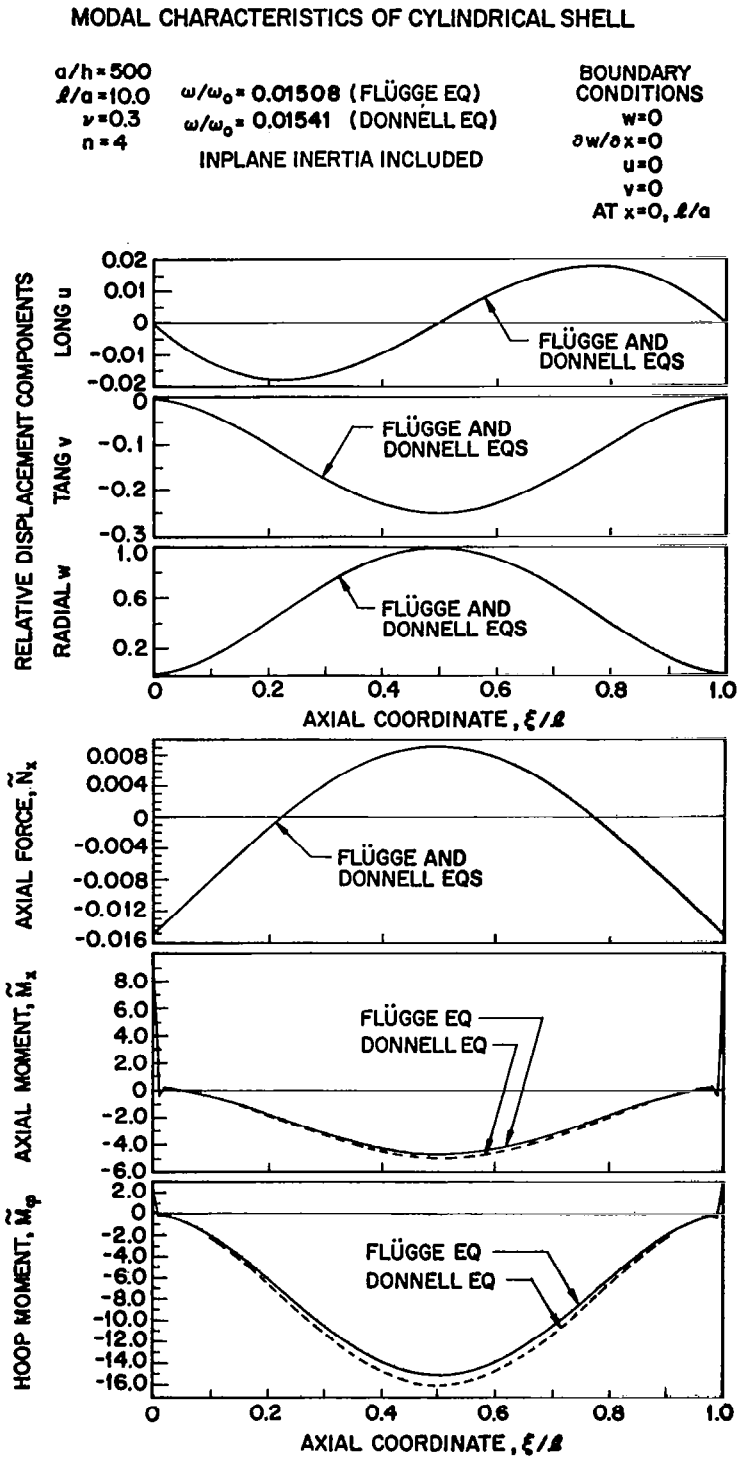

Fig. 8 Comparison of results from Flügge and Donnell Eqs. (including inplane inertia) for mode shape and modal forces (a/h = 500, ℓ/a = 10)

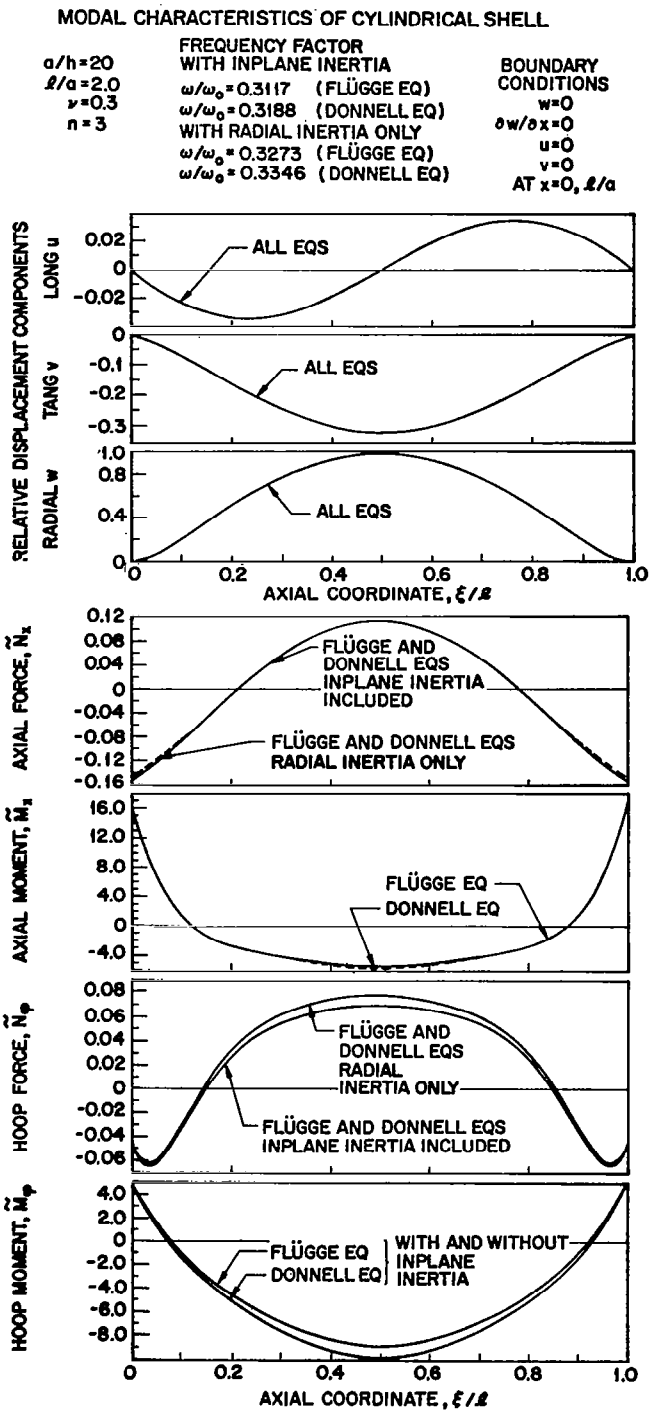

Fig. 9 Comparison of results from Flügge and Donnell Eqs. (with and without inplane inertia) for mode shape and modal forces (a/h = 20, ℓ/a = 2)

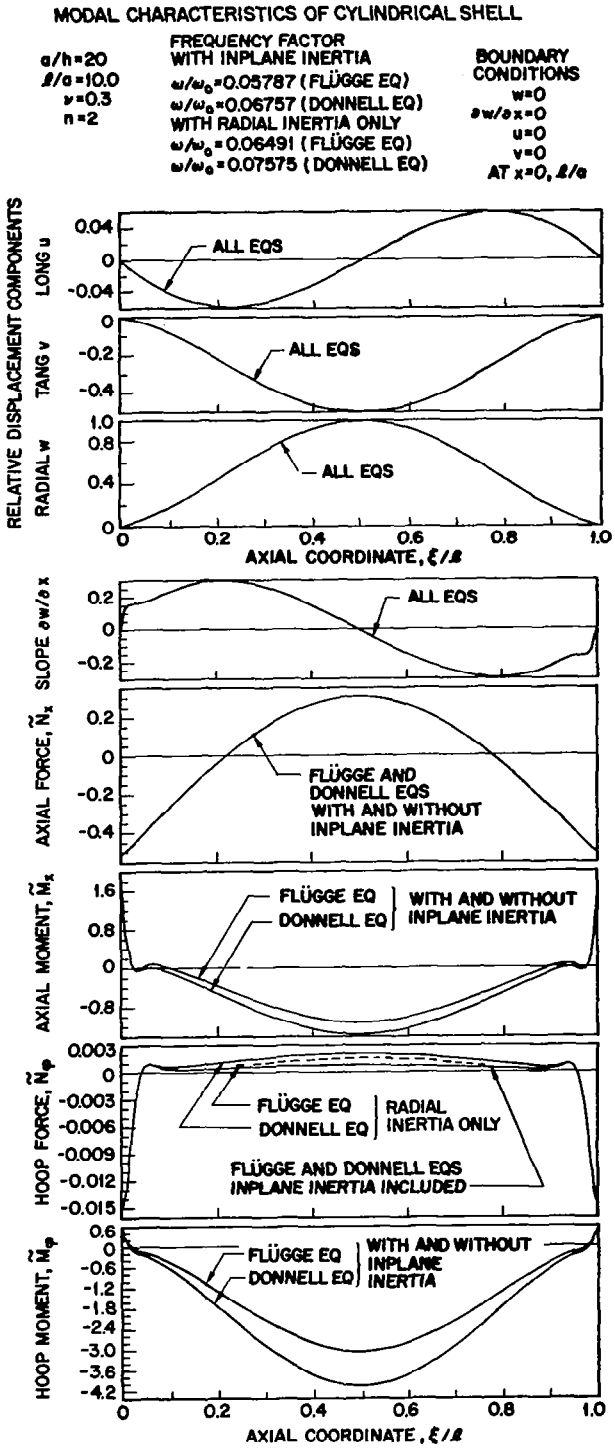

Fig. 10 Comparison of results from Flügge and Donnell Eqs. (with and without inplane inertia) for mode shape and modal forces (a/h = 20, ℓ/a = 10)

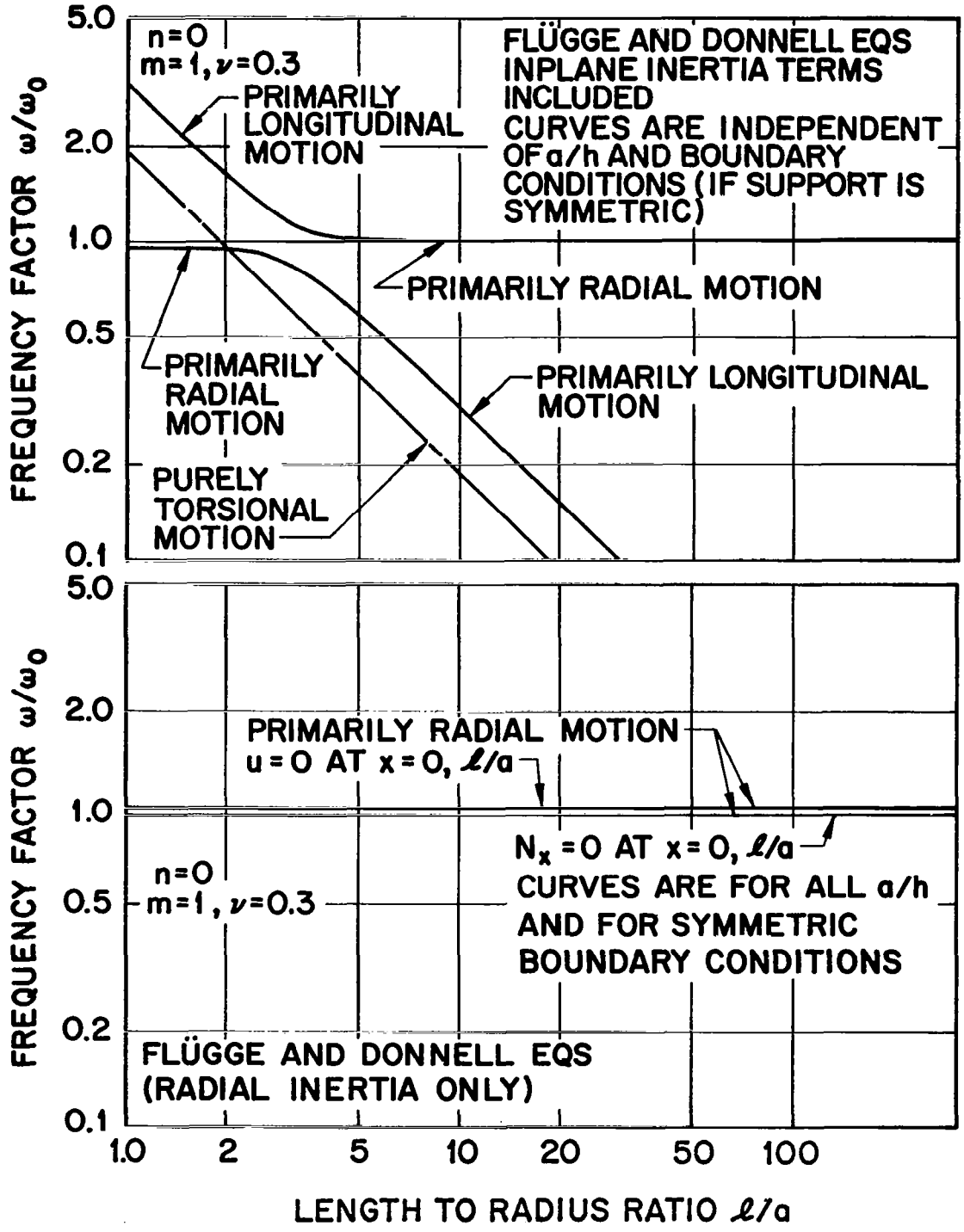

Fig. 11 Effect of inplane inertia terms on axisymmetric mode (n = 0)

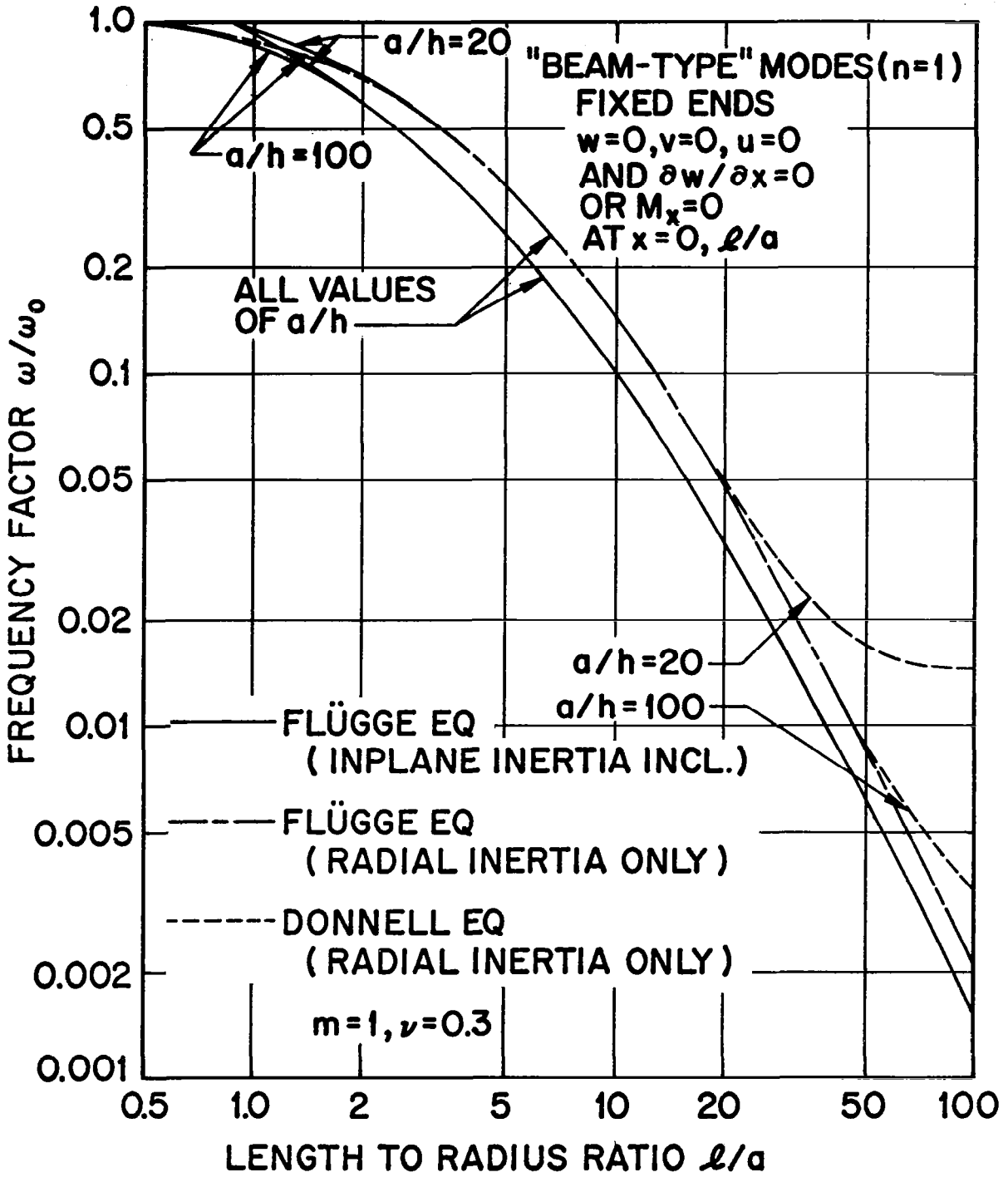

Fig. 12 Effect of inplane inertia terms on "beam-type" mode (n = 1)

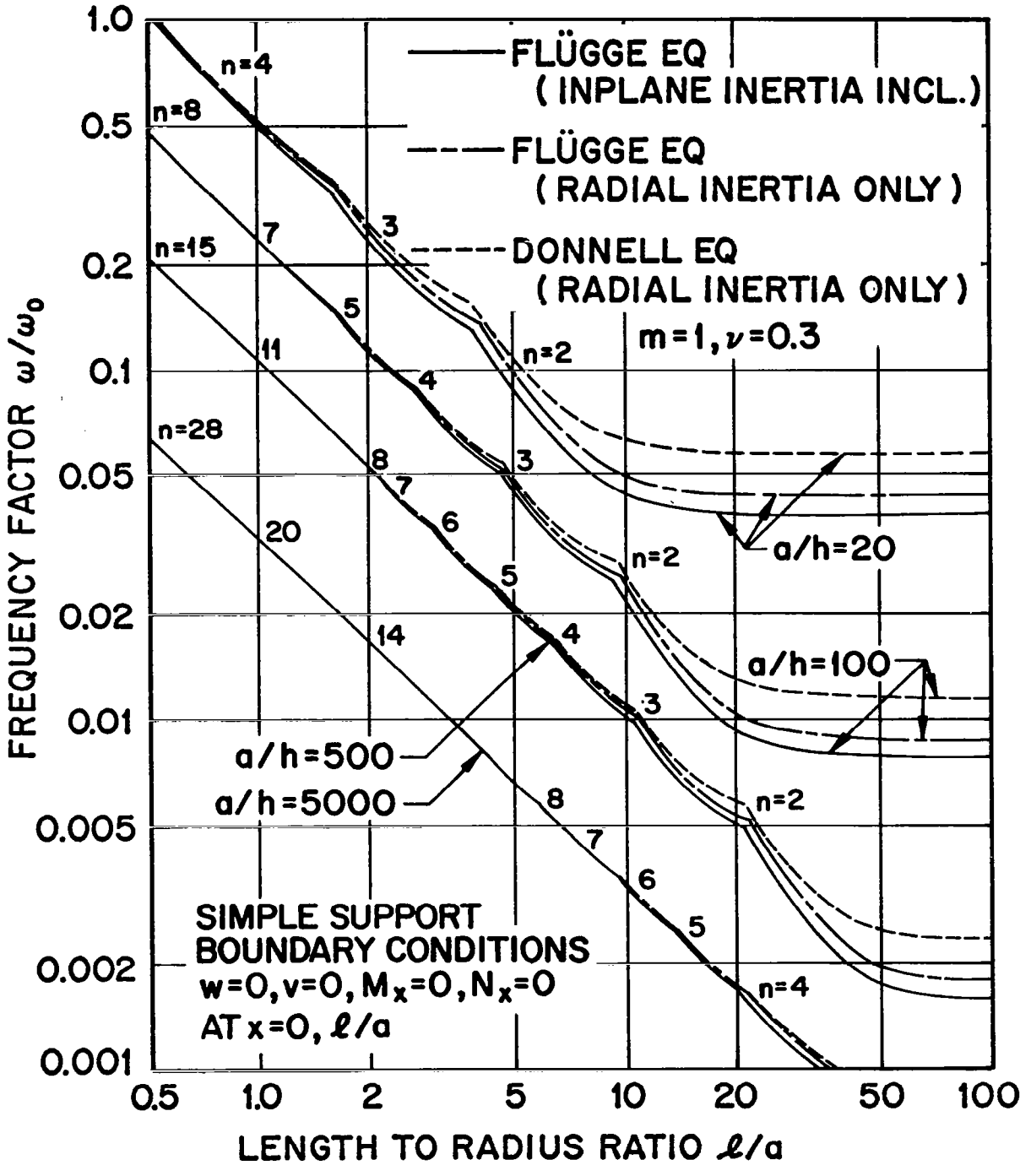

Fig. 13 Frequency envelope, comparing results of Flügge and Donnell Eqs. (with and without inplane inertia) for simple support

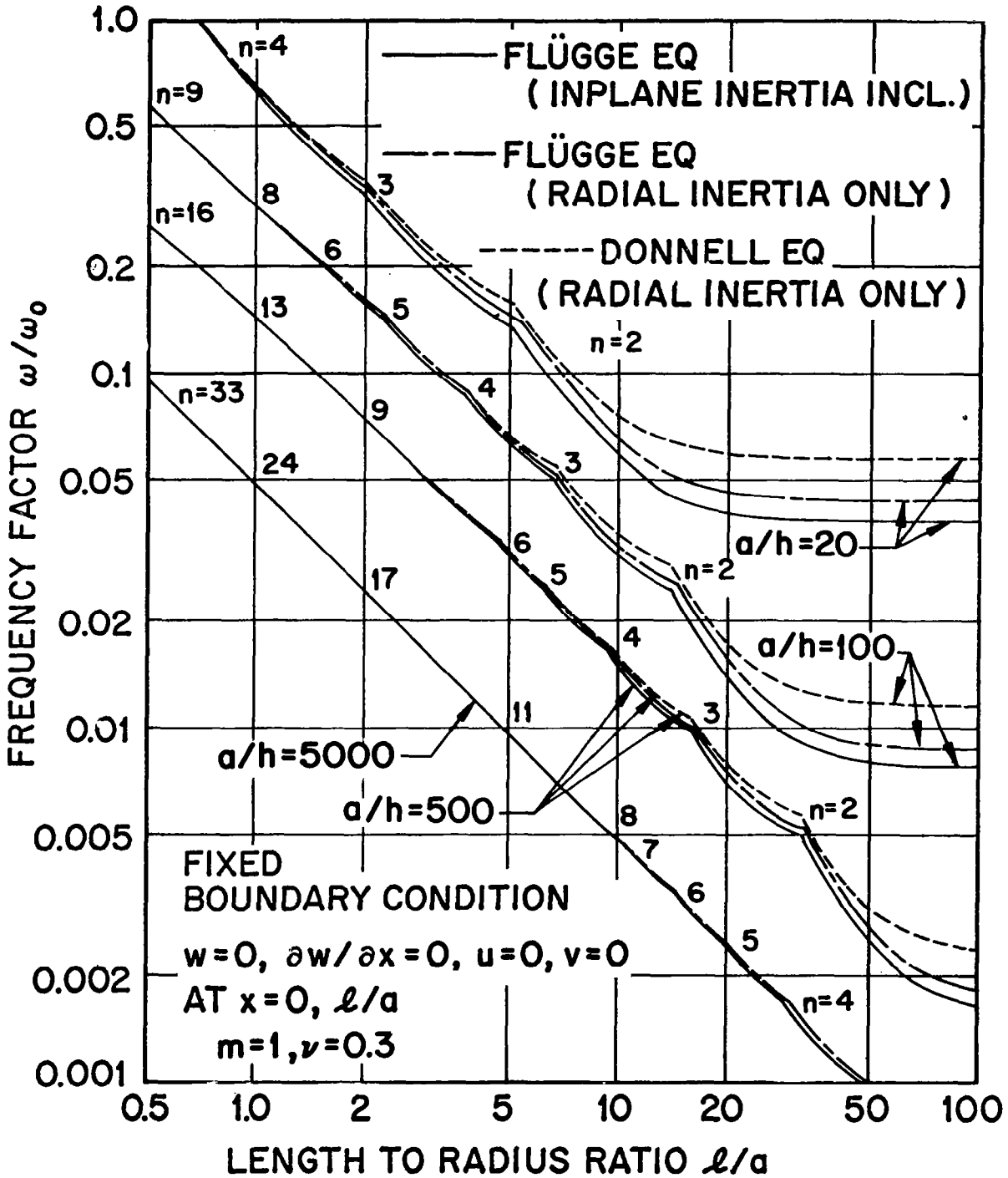

Fig. 14 Frequency envelope, comparing results of Flügge and Donnell Eqs. (with and without inplane inertia) for fixed ends

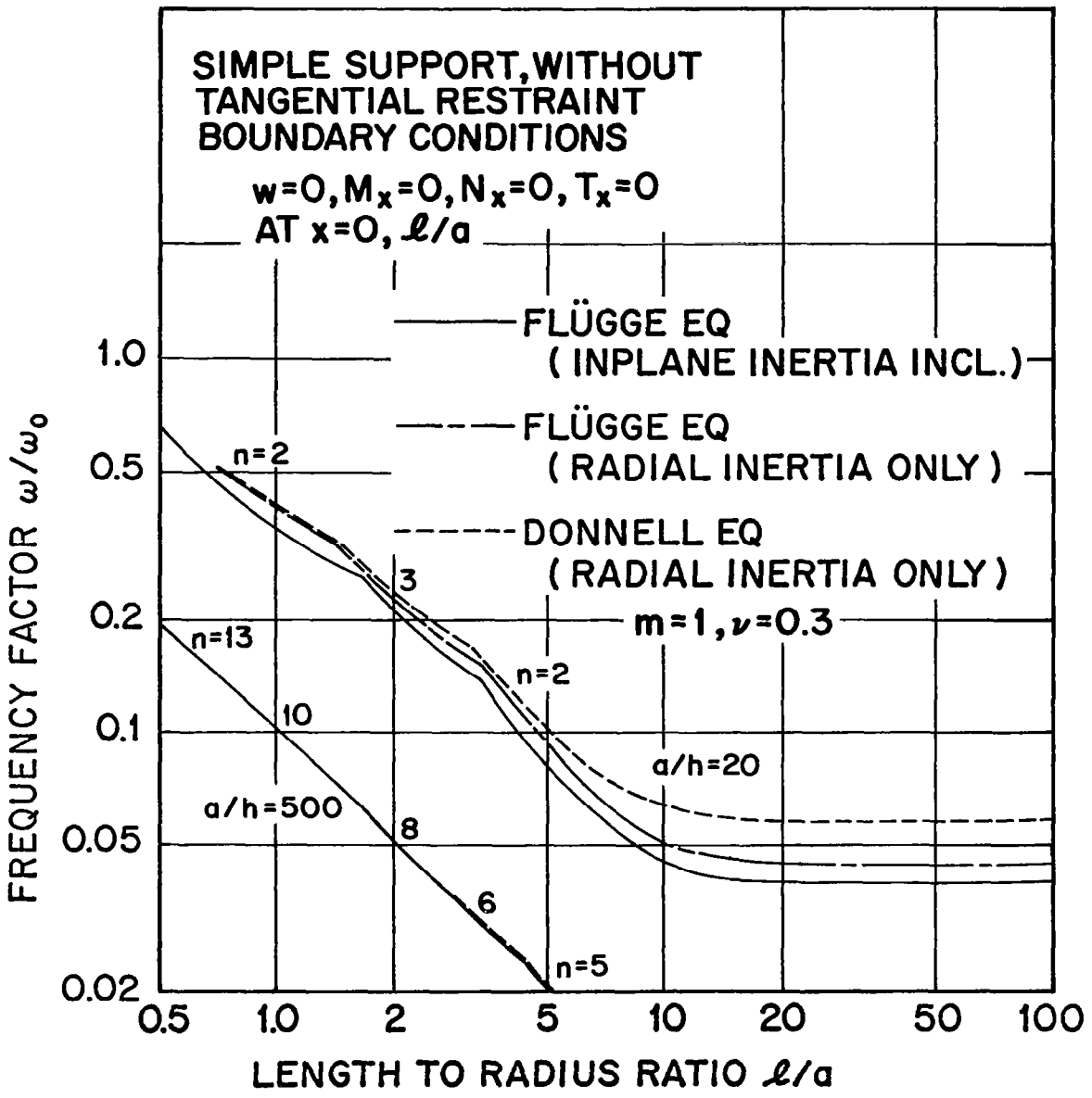

Fig. 15 Frequency envelope, comparing results of Flügge and Donnell Eqs. (with and without inplane inertia) for simple support without tangential restraint

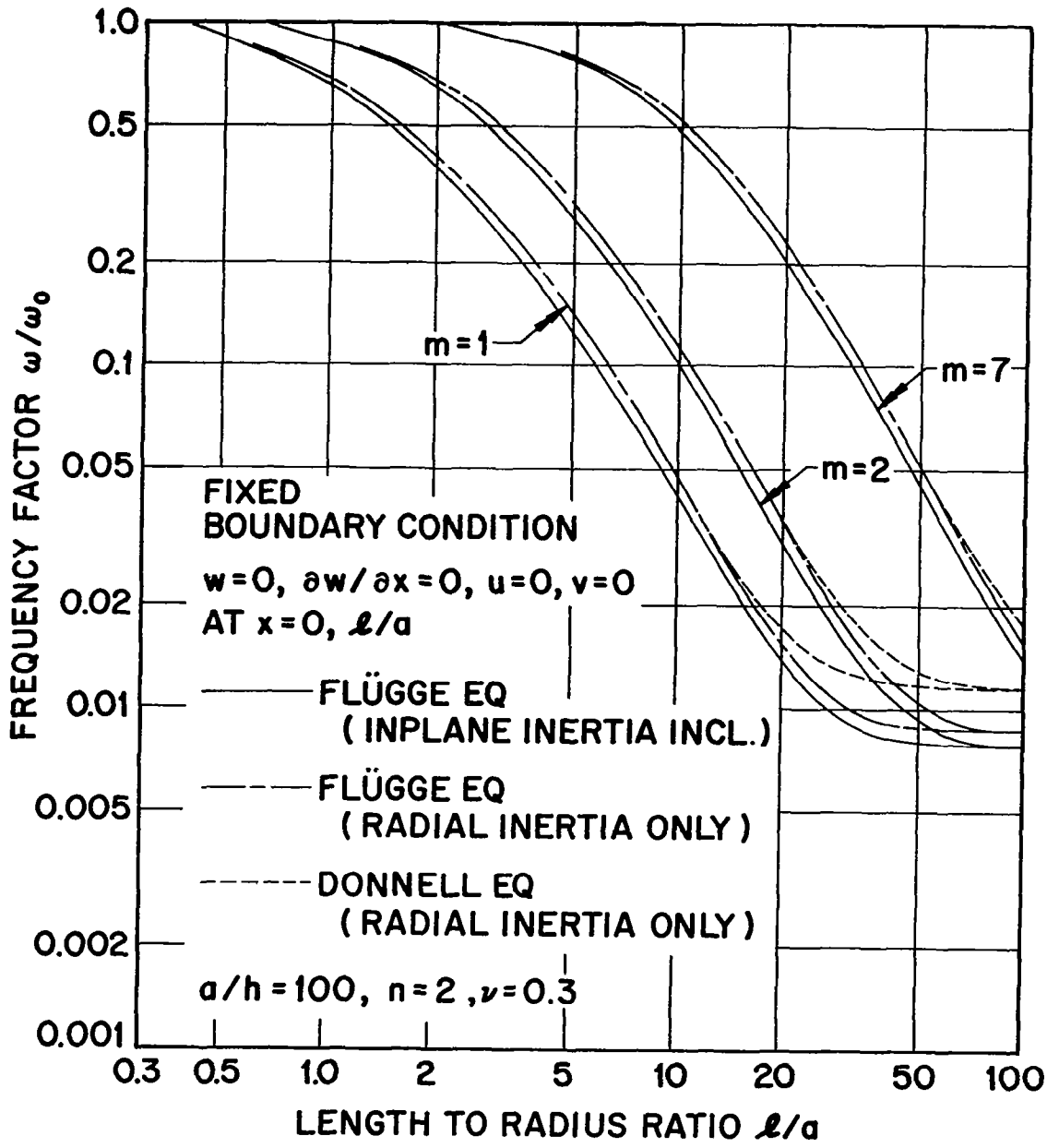

Fig. 16 Frequency spectrum for a/h = 100, n = 2, m ≥ 1, indicating influence of inplane inertia terms

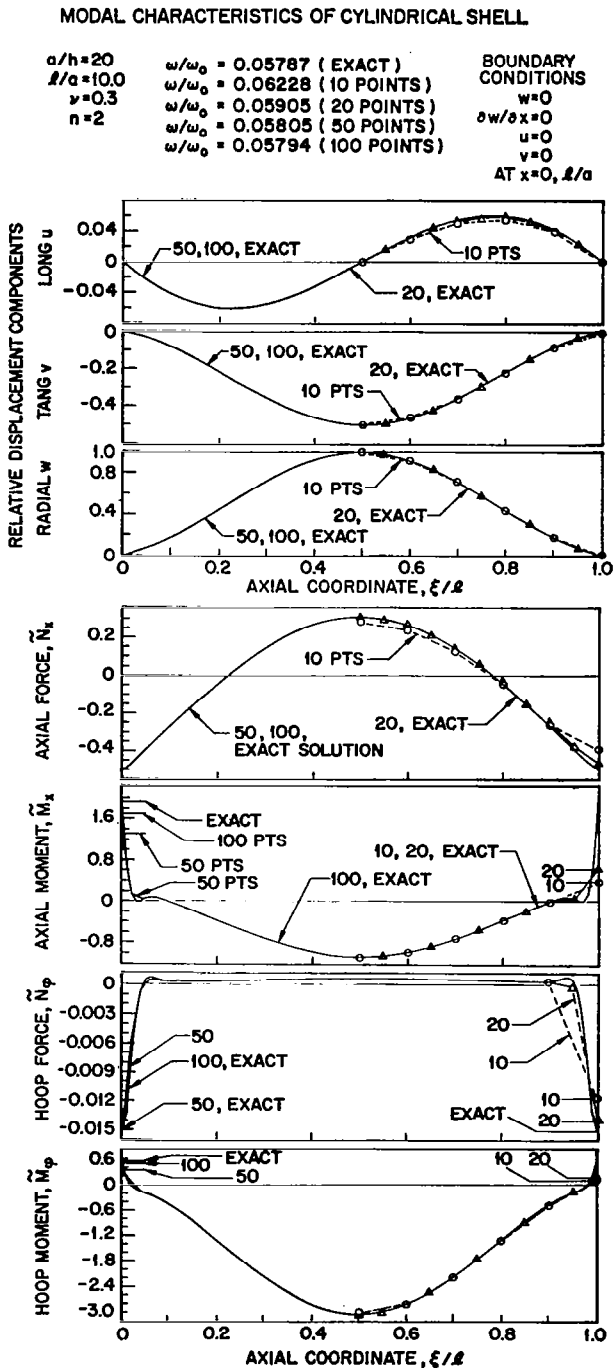

Fig. 17 Comparison of finite difference solution with exact solution for a/h = 20, ℓ/a = 10, n = 2, m = 1; fixed ends

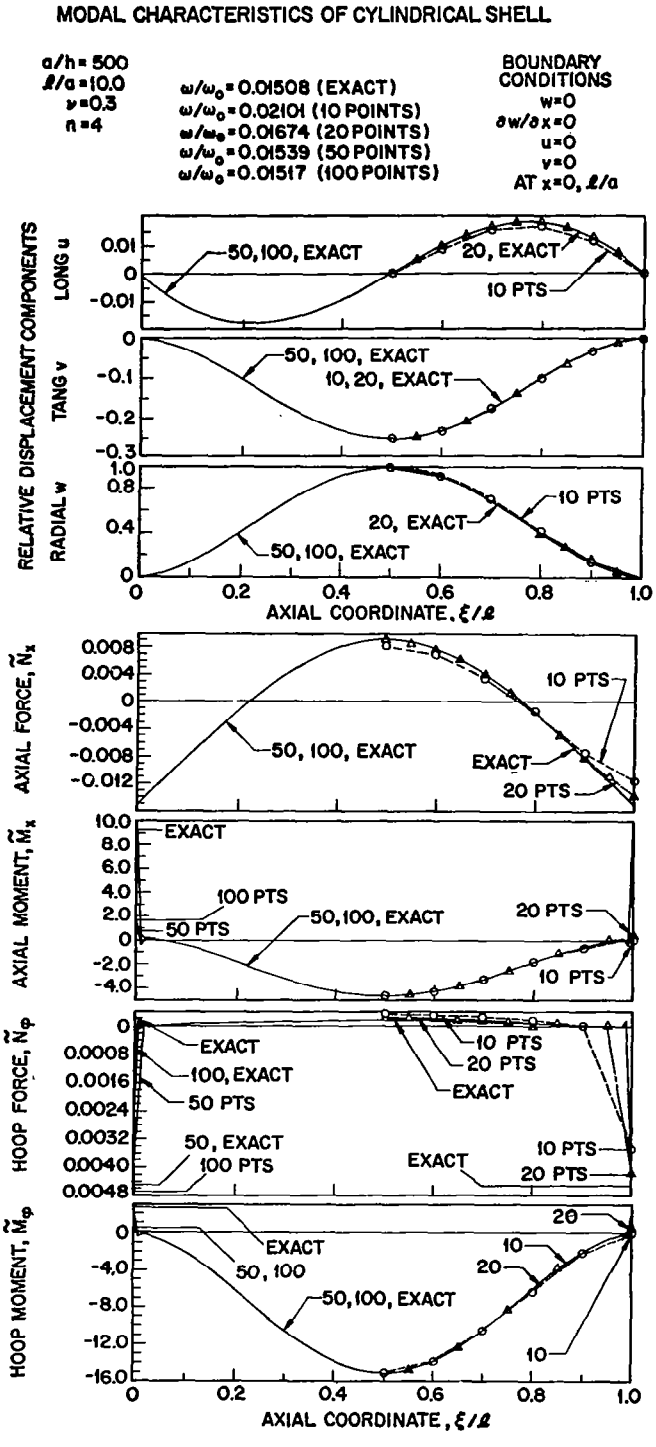

Fig. 18 Comparison of finite difference solution with exact solution for a/h = 500, ℓ/a = 10, n = 4, m = 1; fixed ends

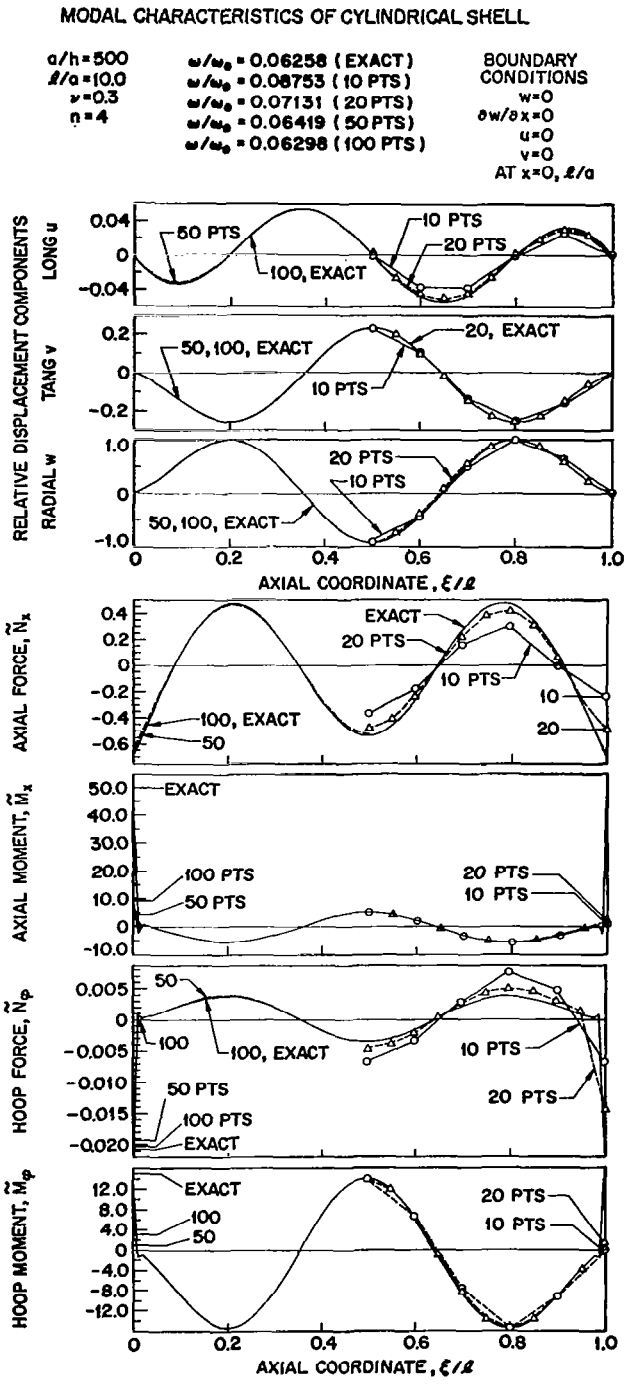

Fig. 19 Comparison of finite difference solution with exact solution for a/h = 500, ℓ/a = 10, n = 4, m = 3; fixed ends

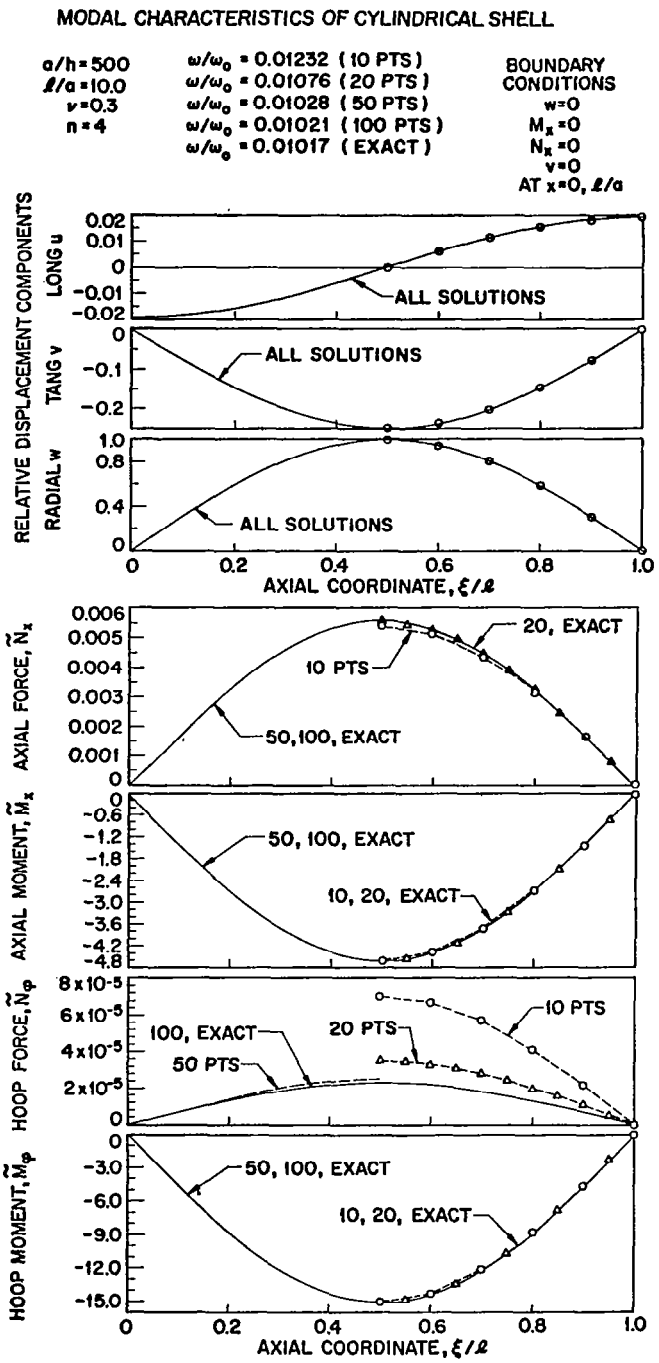

Fig. 20 Comparison of finite difference solution with exact solution for a/h = 500. ℓ/a = 10, n = 4, m = 1; simple support

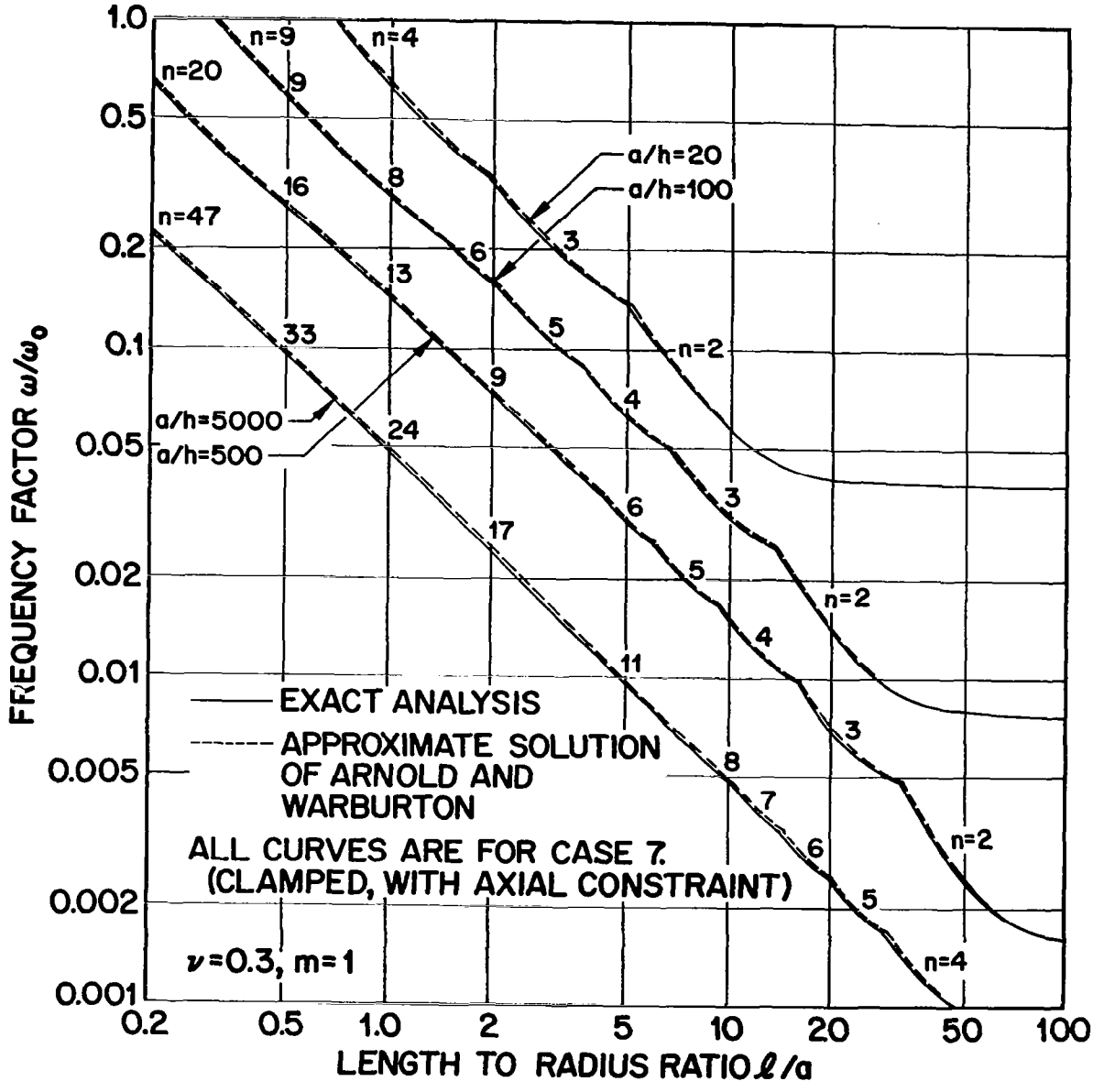

Fig. 21 Frequency envelope, exact solution and Arnold and Warburton's approximate solution

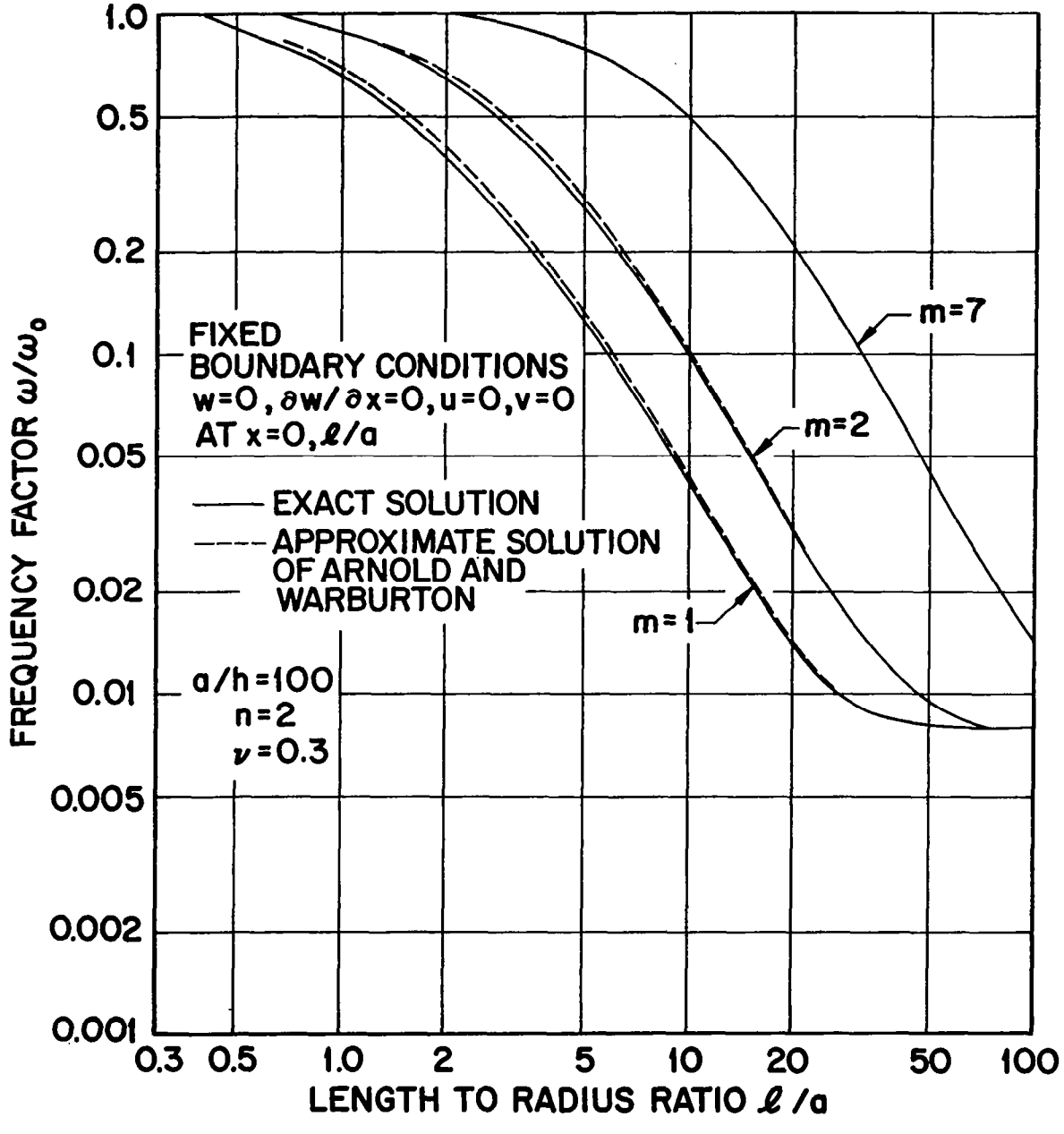

Fig. 22 Frequency distribution for n = 2, m ≥ 1, comparing exact solution and Arnold and Warburton's approximate solution

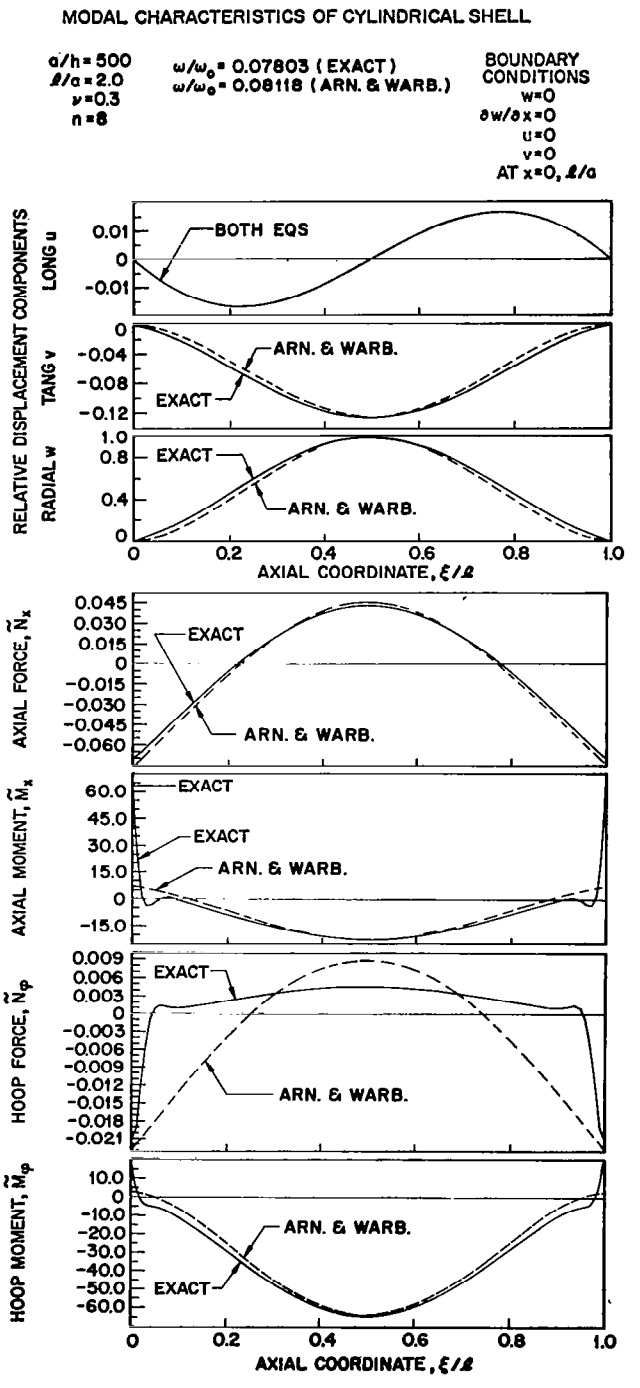

Fig. 23 Comparison of Arnold and Warburton's solution with exact results for a/h = 500, ℓ/a = 2, n = 8, m = 1

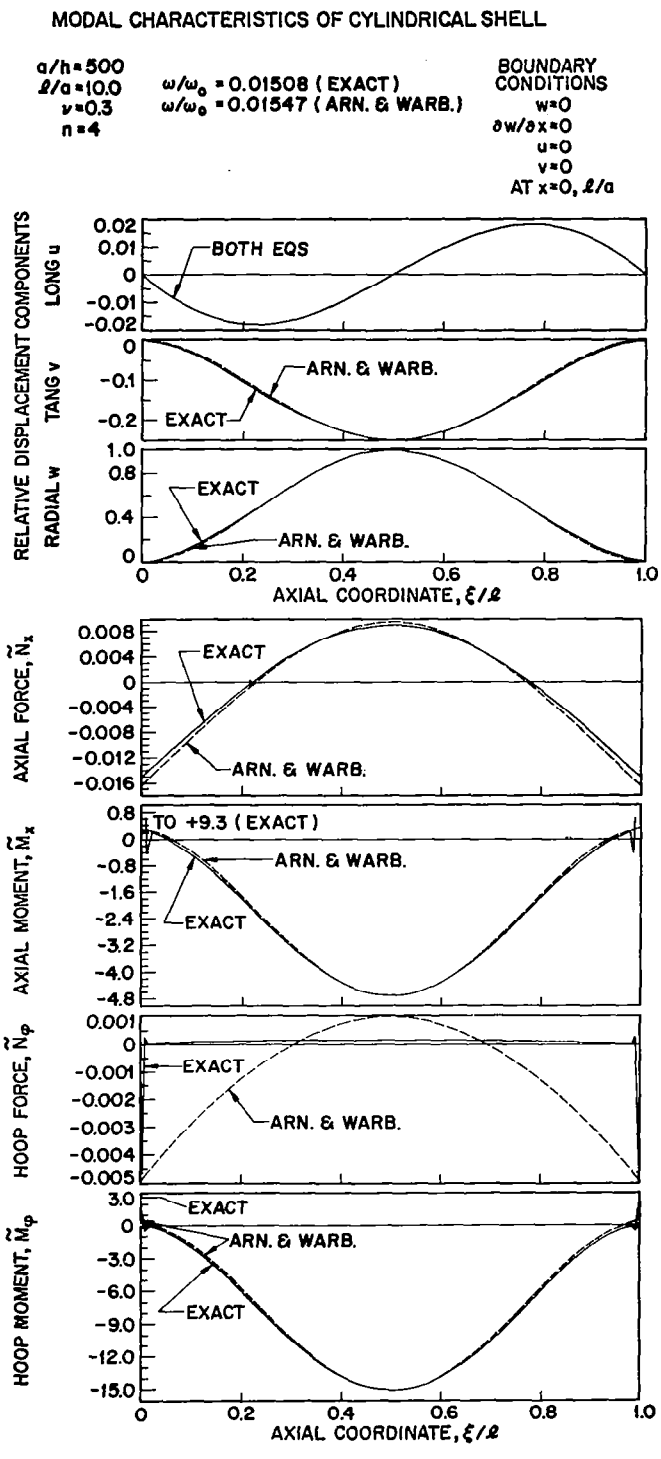

Fig. 24 Comparison of Arnold and Warburton's solution with exact results for a/h = 500, ℓ/a = 10, n = 4, m = 1

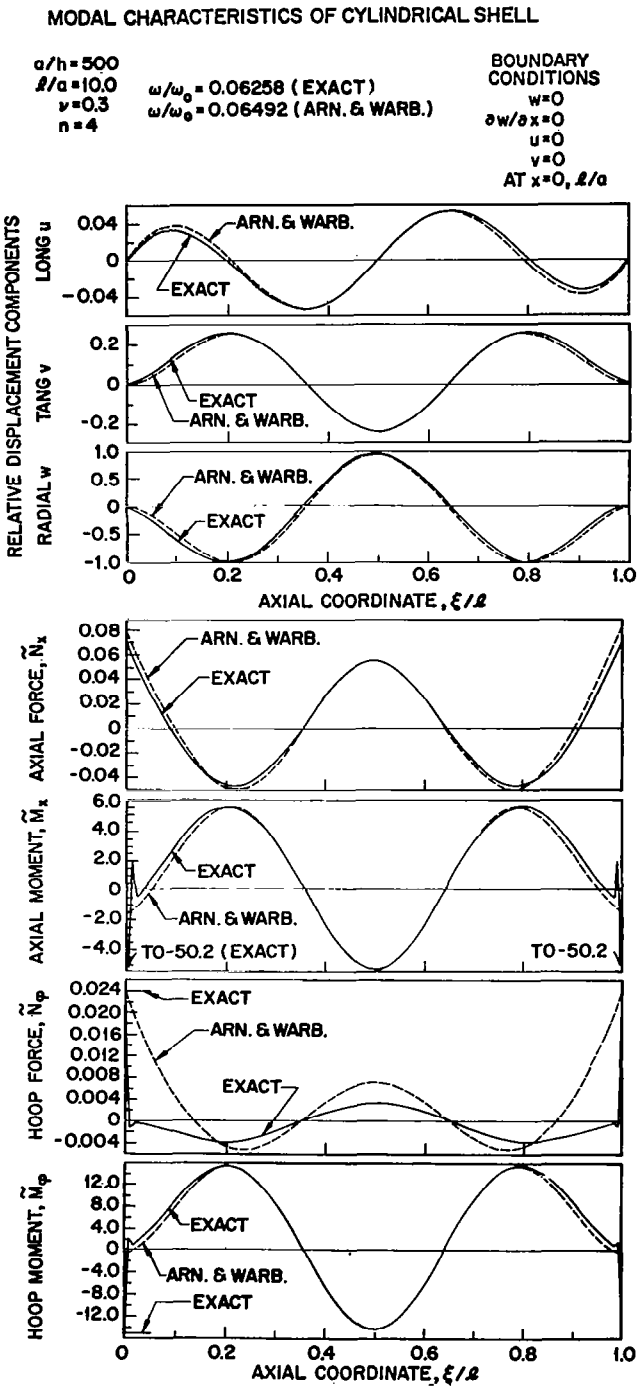

Fig. 25 Comparison of Arnold and Warburton's solution with exact results for a/h = 500, ℓ/a = 10, n = 4, m = 3